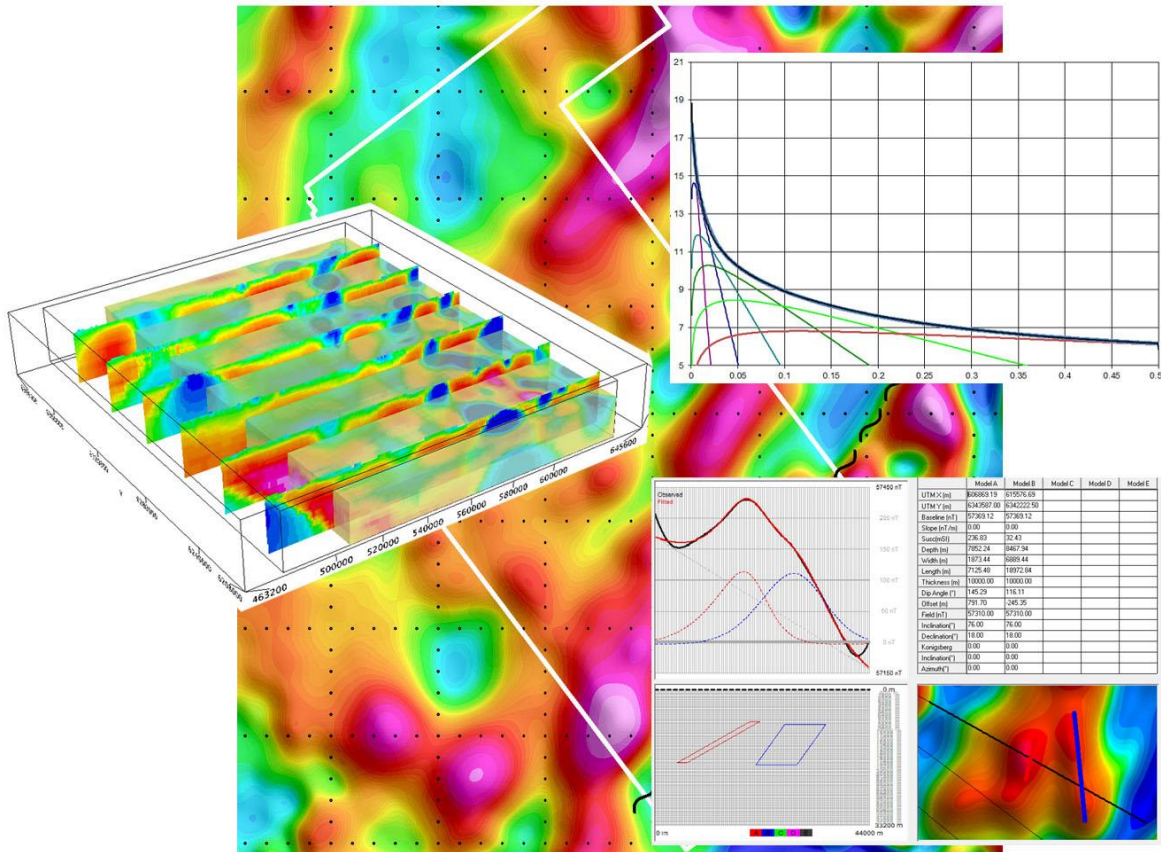


# Geoscience BC Report 2016-17

## Aeromagnetic Data Processing

### Peace Region

### British Columbia



By

**Scott Hogg & Associates Ltd.**

## Table of Contents

1. Introduction .....	2
2. Survey Data .....	2
3. Regional Context .....	3
3.1. GSC Magnetics .....	3
3.2. Geological Atlas of the Western Canadian Sedimentary Basin .....	4
3.2.1. Basement Depth from Oil Well Drilling.....	4
3.2.2. Peace River Arch .....	5
3.2.3. Interpreted Tectonic Domains in the Peace River Region .....	6
4. Data Processing.....	7
4.1. SkyTEM and GSC Regional Data Merge .....	7
4.2. Reduction to Magnetic Pole.....	9
4.3. Depth Slice Filtering .....	9
4.3.1. Expected Basement Layer .....	12
4.3.2. Shallow Magnetic Fraction.....	13
4.4. Calculated Vertical and Horizontal Derivatives.....	17
4.5. Apparent Magnetic Susceptibility.....	17
4.6. Three Dimensional Magnetic Inversion .....	18
4.7. Multi-Mod Magnetic Models.....	20
5. Discussion.....	24
5.1. 3D Inversion .....	24
5.2. Magnetic Model Results .....	28
Appendix I – Digital Products Summary.....	30
Appendix II – Model Report Pages.....	32

## 1. Introduction

The Peace Region of Northeastern British Columbia lies within the western extent of the Western Canadian Sedimentary Basin (WCSB). The WCSB is characterized as a wedge-shaped layer of sedimentary rock that is greater than three kilometers thick at the Rocky Mountains in the west and tapers to zero thickness at its Eastern boundary with the Canadian Shield. The basin is host to one of the World's largest reserves of petroleum and natural gas.

Throughout the past several decades, the oil and gas industry has explored much of the WCSB and has indirectly provided insight into the nature of the Precambrian basement that lies underneath. Through exploratory drilling, the thickness of the sedimentary section is generally quite well mapped in much of the western zone of the WCSB, but the Peace Region of BC is not as well known.

In an effort to better map the ground water in the Peace Region, a helicopter-borne magnetic and electromagnetic survey was carried out by SkyTEM Surveys in the summer of 2015. The following report describes processing methodologies and an interpretation of the magnetic data to map the crystalline basement.

This report was prepared through the support of Geoscience BC<sup>1</sup>.

## 2. Survey Data

The survey was a helicopter-borne magnetic and transient electromagnetic survey. The electromagnetic data has been excluded from this investigation. The nominal terrain clearance of the magnetic sensor was 50 metres. Traverse lines were flown at a 50°-230° azimuth and spaced 600 metres apart. A total of 20,337 kilometers of data was collected.

In the contractor's final magnetic profile channel, shallow detail had been largely stripped away. Much of the shallow detail was cultural in origin, but it is likely that some detail arising from shallow geological features was also removed.

---

<sup>1</sup>Geoscience BC is an independent, non-profit organization that generates earth science in collaboration with First Nations, local communities, government, academia and the resource sector. Our independent earth science enables informed resource management decisions and attracts investment and jobs. Geoscience BC gratefully acknowledges the financial support of the Province of British Columbia.

### 3. Regional Context

#### 3.1. GSC Magnetics

Regional aeromagnetic data is available from the Geological Survey of Canada in the form of a 200m seamless grid that covers the entire country. The figure below shows a subset of the GSC data, with the Peace Region survey outline in green.

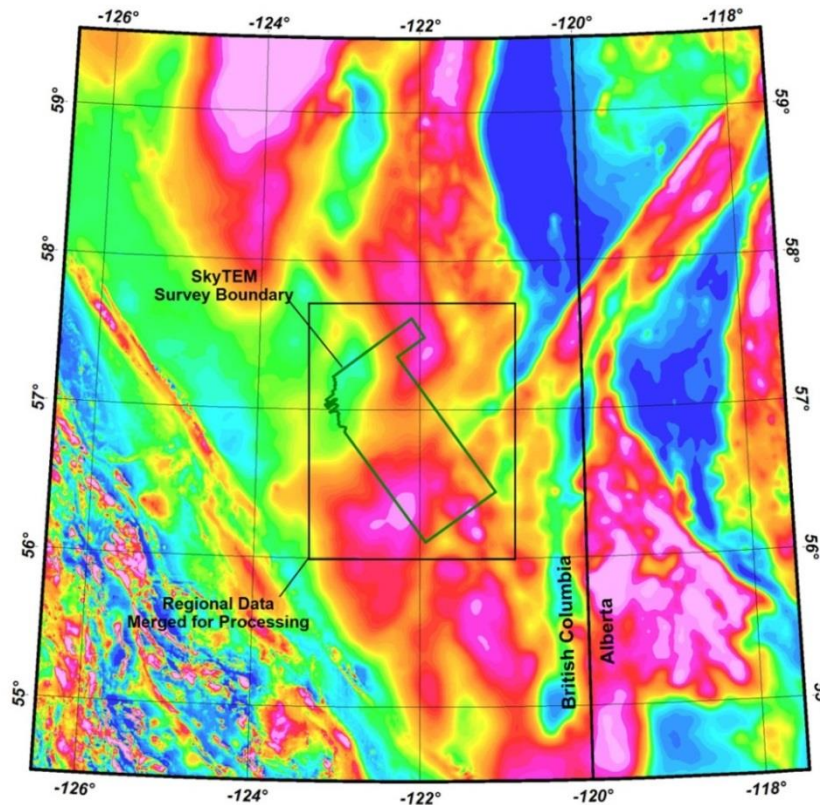


Figure 1 – Regional Total Magnetic Field

A regional data subset, bounded by the black rectangle in the figure, was extracted and merged with the SkyTEM data for processing. See section 4.1.

### 3.2. Geological Atlas of the Western Canadian Sedimentary Basin

The maps in this section are taken from the Geological Atlas of the Western Canada Sedimentary Basin; Canadian Society of Petroleum Geologists and Alberta Research Council [Mossop, G.D. and Shetsen, I., comp. (1994)].

#### 3.2.1. Basement Depth from Oil Well Drilling

As a consequence of extensive oil and gas exploration, the depth to the Precambrian basement is well defined by drill results in the Province of Alberta. Drill well locations are indicated on the map below and depth to basement contours have been interpolated. The contours have been extrapolated partway into the Peace survey area, but there does not appear to be any well locations plotted within the survey.

Basement depths exceeding four kilometers and approaching six kilometers are expected in the eastern portion of the surveyed area. Note that the Cordilleran Deformation Zone has been interpreted as passing through the survey area.

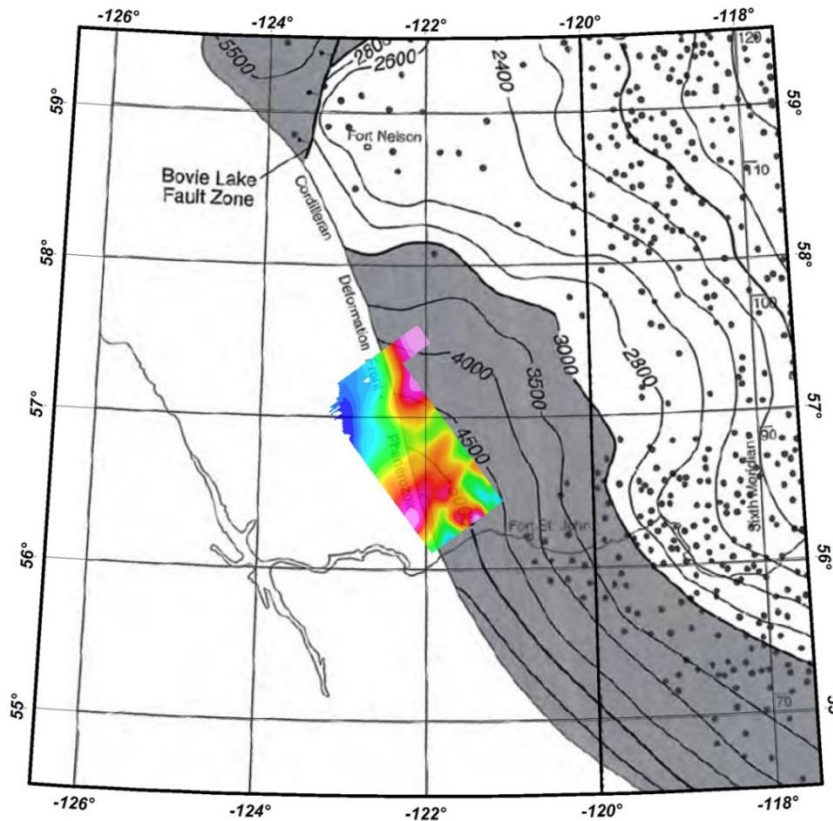


Figure 2 – Basement Depth from Oil Well Data

### 3.2.2. Peace River Arch

The Peace River Arch is a major uplift of the Precambrian basement within the western extent of the WCSB. The image below shows basement depth contours defined by oil well drilling data in the province of Alberta. Approximate north and south limits of the arch are symbolized by heavy dashed lines. The position of the SkyTEM survey data is shown off to the west of the contour map. It is possible that the arch extends further west into the southern end of the survey.

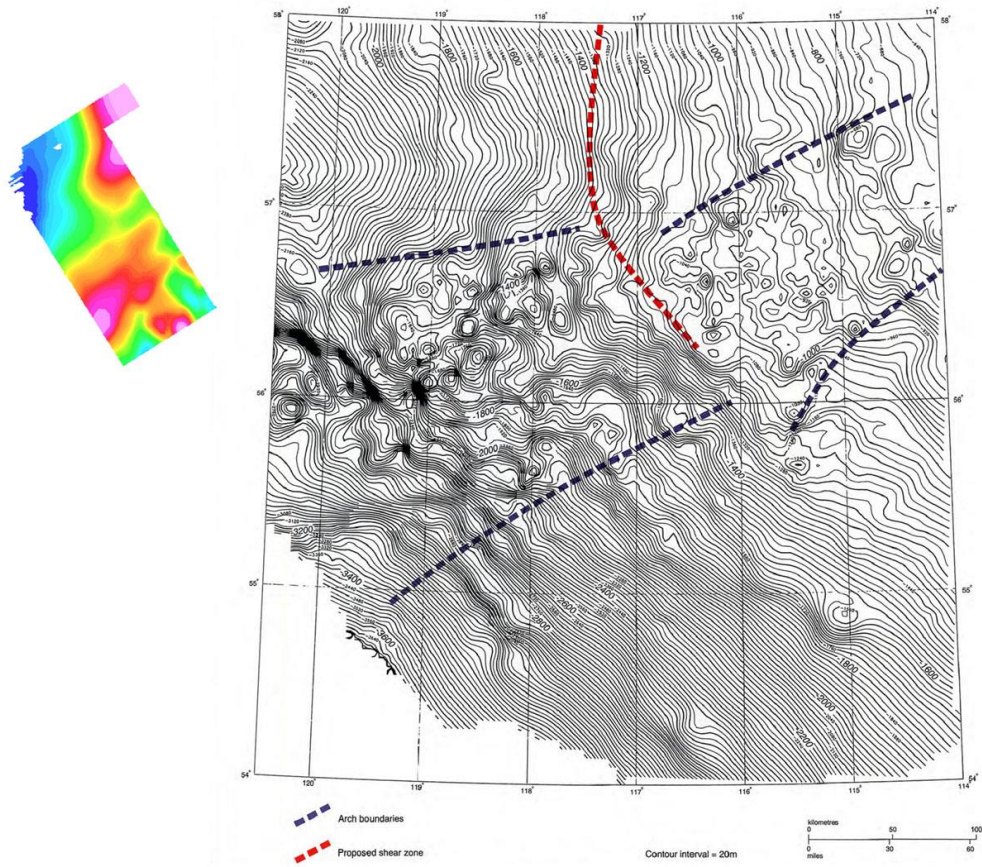


Figure 3 – Peace River Arch Basement Contours

### 3.2.3. Interpreted Tectonic Domains in the Peace River Region

Regional aeromagnetic data has been interpreted and major tectonic domains of the basement are shown in the image on the following page. The SkyTEM survey data is included.

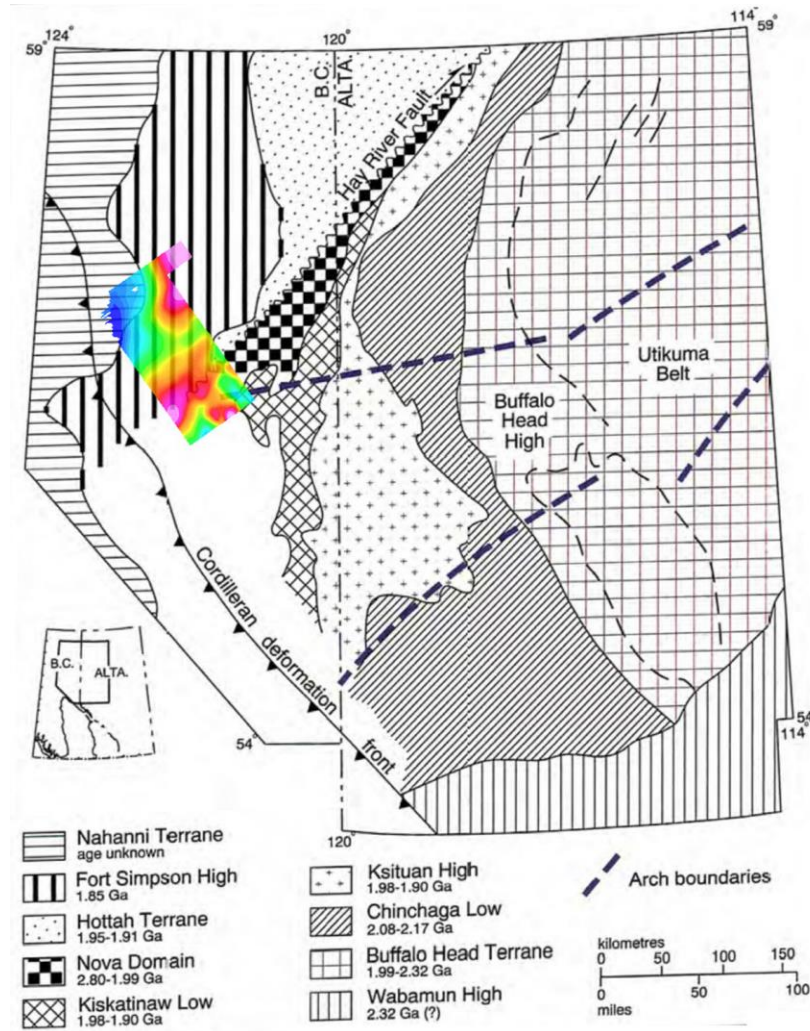


Figure 4 – Tectonic Domains in the Basement of the Peace River Region

The survey straddles the southern end of the Fort Simpson high, and the Hay River fault extends into the area. This interpretation extends the northern boundary of the Peace River Arch into the SkyTEM survey area. Note that the Cordilleran Deformation Front has been interpreted to lie west of the survey area, rather than through it as shown in Figure 2.

The image below shows a portion of the tectonic interpretation with the magnetic data.

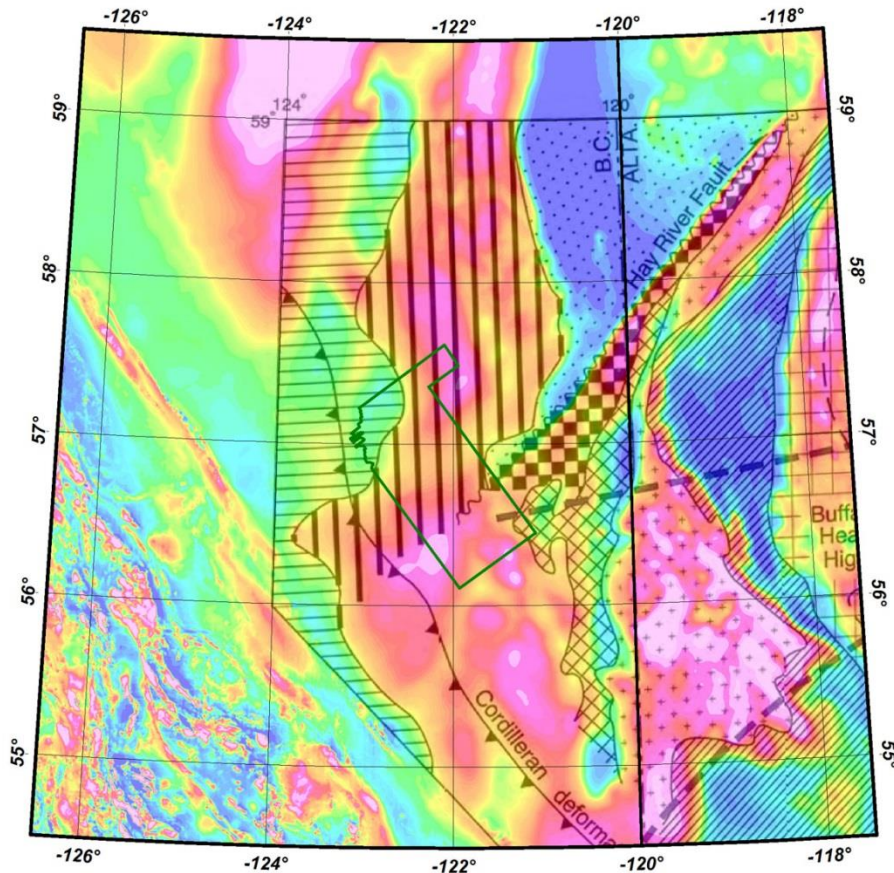


Figure 5 – Regional Tectonic Interpretation and Mag

## 4. Data Processing

### 4.1. SkyTEM and GSC Regional Data Merge

The processing outlined in this report is largely aimed at investigating depth. To quantify magnetic sources at great depth, it is necessary that the magnetic dataset have sufficient horizontal extent. By padding the SkyTEM data with regional data, the frequency content of the compilation can include components with very long wavelength. Furthermore, with the inclusion of regional data outside the limits of the SkyTEM survey, a broader context is provided and any edge effects introduced by the processing will be kept outside the area of primary focus.

The GSC data has been compiled from a number of different airborne surveys, flown over a period of several decades. The figure below shows the extent of the regional subset used in the data merge, with the SkyTEM survey outline shown in blue. Where available, the original regional survey flight lines are included. Pseudo magnetic profile data from the original surveys has been recovered by digitizing contour intercepts from paper maps, but the original survey data is not readily available.

Sheet boundaries of the National Topographic System (NTS) are shown as grey lines in this figure, subsequent figures in this report and all maps accompanying this report. The Dominion Land Survey (DLS) system is defined in the southeast corner of the area and is represented with dashed, black lines. The coordinate system is WGS84, UTM Zone 10N.

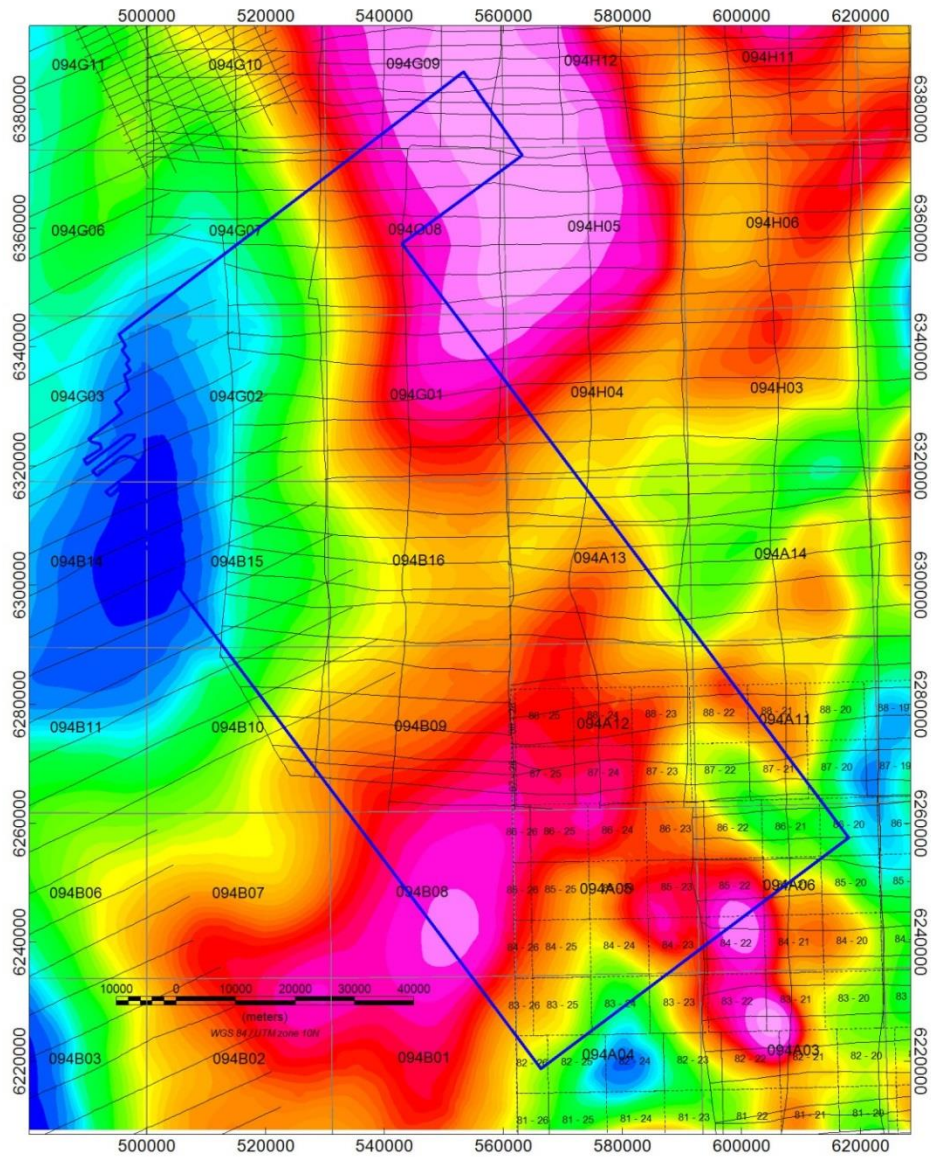


Figure 6 – Regional GSC Mag with Original Flightpath

When the GSC merged all of the various datasets to produce the seamless country-wide grid, long-wavelength corrections were made to the gridded data to bring them all to a common datum. Metadata available from the GSC suggests that the surveys used in the compilation for this report were all flown using a 300m altitude drape surface. It is unknown what leveling corrections were applied to various datasets.

As a first step in merging the GSC data with the SkyTEM data, the GSC data was downward continued by 250m to bring it closer to the elevation of the SkyTEM survey. A level correction was then applied to the sharpened GSC gridded data. The correction used had a DC component to restore the total magnetic field to the residual, regional data. In addition to the DC component, a long wavelength correction was also applied. The wavelength of the correction was controlled by a half cosine roll-off filter (20km to 10km).

## 4.2.Reduction to Magnetic Pole

The anomaly shape associated with a vertically dipping magnetic source varies with the inclination of the earth's magnetic field. At the north and south magnetic pole, the inclination is vertical and the anomaly is positive, symmetrical and centered directly over the source. At the equator, with a horizontal inducing field, the anomaly is negative, symmetrical and centered directly over the source. Between 0 and 90 degrees of inclination the anomaly is asymmetric, with a positive and negative component, and is not centered over the source. The pole reduction process reshapes the anomaly measured at intermediate inclinations to resemble the shape that would have been measured at vertical inclination. Thus a steeply dipping source, without remanent magnetization, would be transformed to a simple positive peak above the source.

The gridded data was reduced to the magnetic pole using a Fourier transform filter.

## 4.3.Depth Slice Filtering

The Fourier Transform,  $A_n(\mathbf{f})$ , of a magnetic source, is expressed by the following exponential function of depth  $\mathbf{d}$  and thickness  $\mathbf{t}$ , with respect to radial frequency ( $\mathbf{f}$ ).

$$A_n(\mathbf{f}) = S_n e^{-\mathbf{d}(2\pi\mathbf{f})} (1 - e^{-\mathbf{t}(2\pi\mathbf{f})})$$

The coefficient;  $S_n$  is a function of the magnetic susceptibility, size and dip of the body, as well as the inclination, declination and strength of the earth's magnetic field.

As the thickness becomes very large, the term  $e^{-\mathbf{t}(2\pi\mathbf{f})}$  approaches zero and one finds the special case of infinite depth extent:

$$A_b(\mathbf{f}) = S_b e^{-\mathbf{d}(2\pi\mathbf{f})}$$

In the Fourier domain, the spectral signatures of each magnetic component, contributing to the total magnetic field, are combined. If a number of sources are at a common depth, with the same depth extent, a plot of the natural logarithm of the power spectrum, with respect to radial frequency ( $f$ ), may display a linear section relating to the layer.

The merged (detail and regional) total magnetic field Peace Region grid described above was transformed into the frequency domain. The image below shows the natural logarithm of the radially averaged amplitude spectrum of the data.

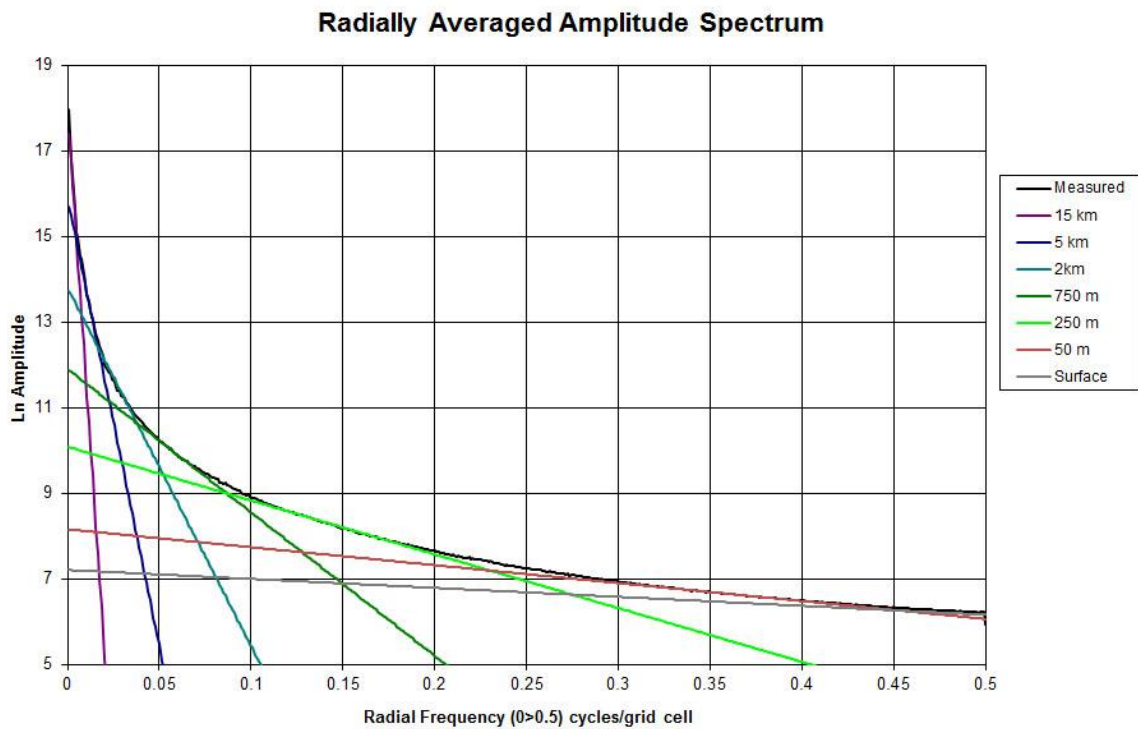


Figure 7a – Amplitude Spectrum and Interpreted Depth Tangents

The spectrum does not display a simple depth segregation, but some suggestions of linear segments have been identified, representing specific depths.

The figure on the following page shows the spectral contribution of each layer and the numeric sum of all the layers, compared to the measured data. The amplitudes of each layer of the model were calculated individually and added as total amplitude. The amplitude scaling factors, for each model layer, were adjusted so the total model amplitude matched the actual amplitude calculated for the grid.

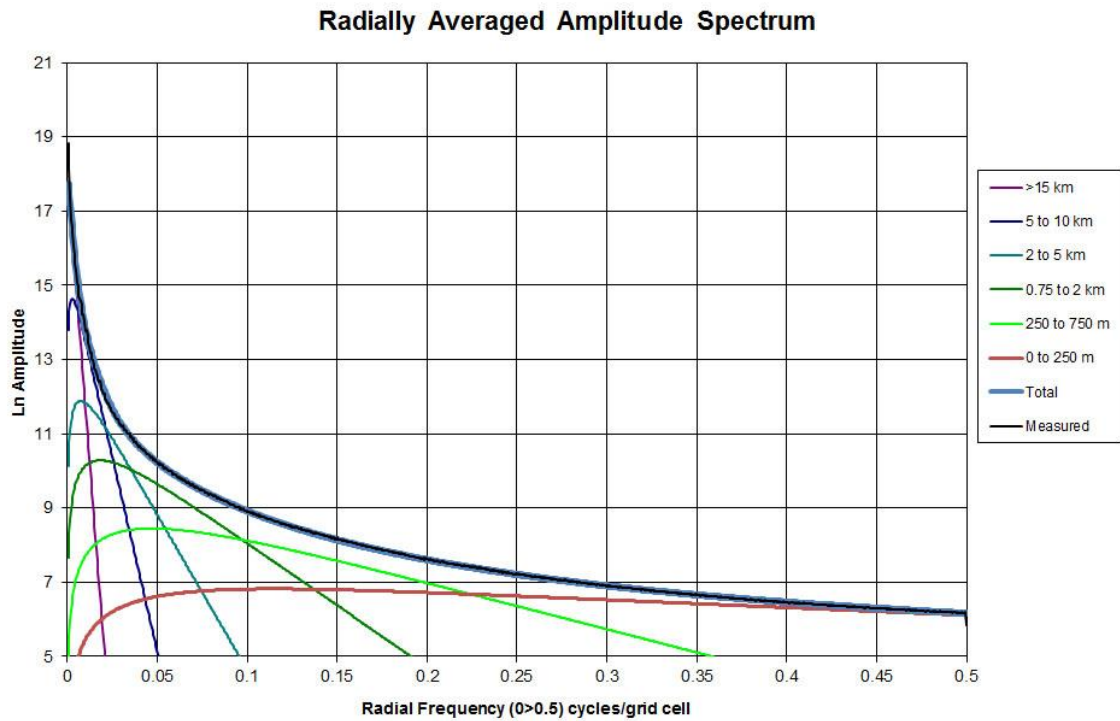


Figure 7b – Amplitude Spectrum with Spectral Components of Layers

A filter was created to isolate the magnetic contribution from the various layers. Four depth slice grids have been produced and are included with this report, along with the pole-reduced total magnetic field grid. The depth slice grids are:

- Greater than 15 km
- 5km to 15km
- 2km to 5km
- Top 2km\*

\* The top layer will exclude magnetic anomalies due to surface and near surface sources, as this detail has been largely removed from the final total magnetic field data by the survey contractor.

### 4.3.1. Expected Basement Layer

Analysis of the amplitude spectrum indicated a very deep layer (>15km depth) which may be representative of a deep, sub-basement. Another layer, originating at 5000m depth is believed to represent the top of the crystalline basement. The figure below shows the pole-reduced residual magnetic field grid of the layer. A vertical derivative grid (CVG) was calculated from the RMI grid and contour lines, where the CVG grid has zero value, were drawn over the RMI grid. The zero CVG contour accentuates contacts. Some possible faults have been interpreted that trace edges of basement units or boundaries enclosing several units. Additional fault lines have been drawn along alignments of possible fault displacements of magnetic axes. A potential extension of the Hay River Fault has been labeled.

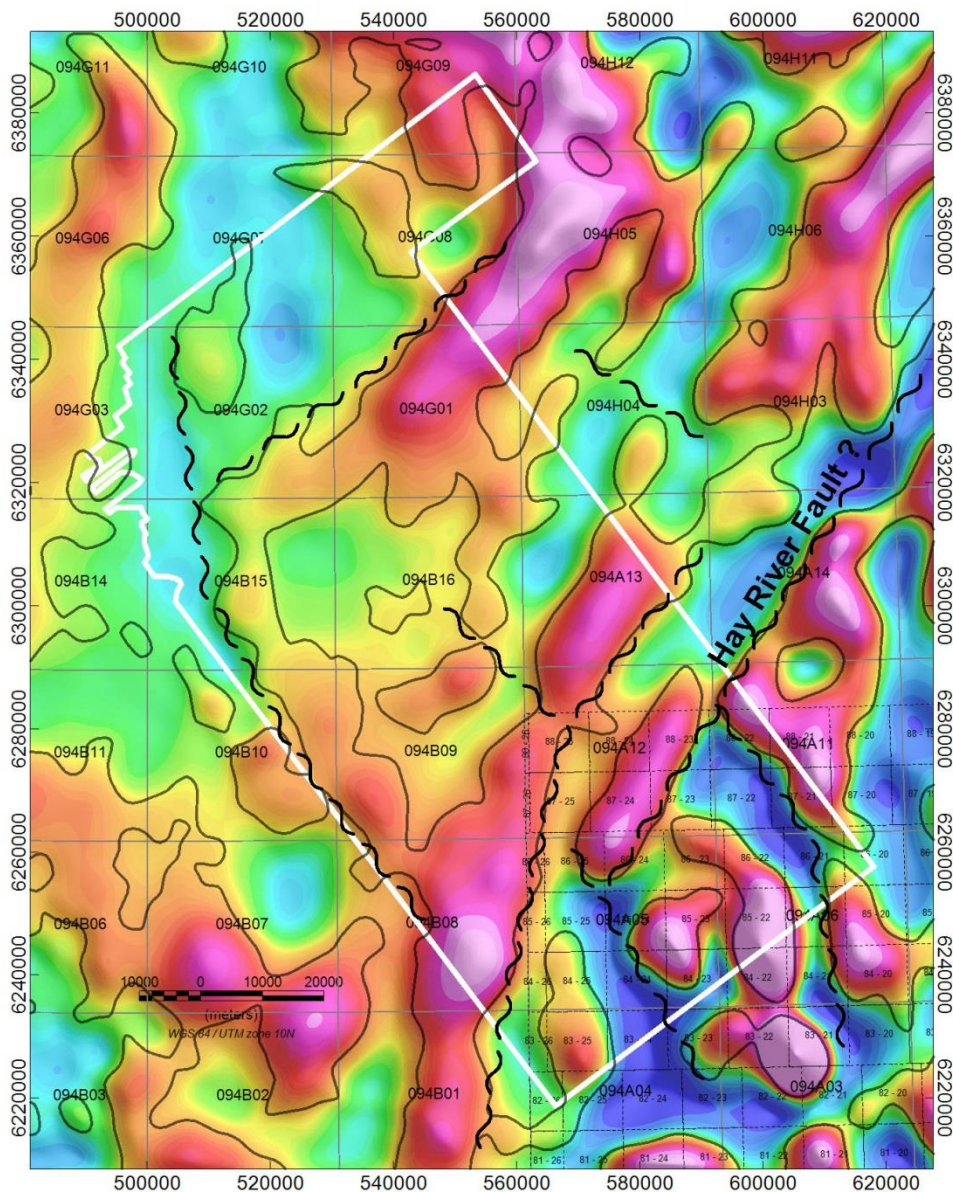


Figure 8 – Residual Magnetic Field at 5000m Depth

### 4.3.2. Shallow Magnetic Fraction

The image below shows the magnetic content representing the top 2000m of lithology. Very near-surface magnetic detail is not present, as it has been removed by the contractor. The colour range in the grid is +/- 2.5 nT and the SkyTEM survey boundary is shown as a white line. The layer illustrates some levelling deficiencies in the survey data (in the zone spanned by lines 11700 to 11800, noted in the figure), as well as gridding artifacts and noise in the GSC data. The varied sample intervals in the surveys comprising the regional compilation are apparent.

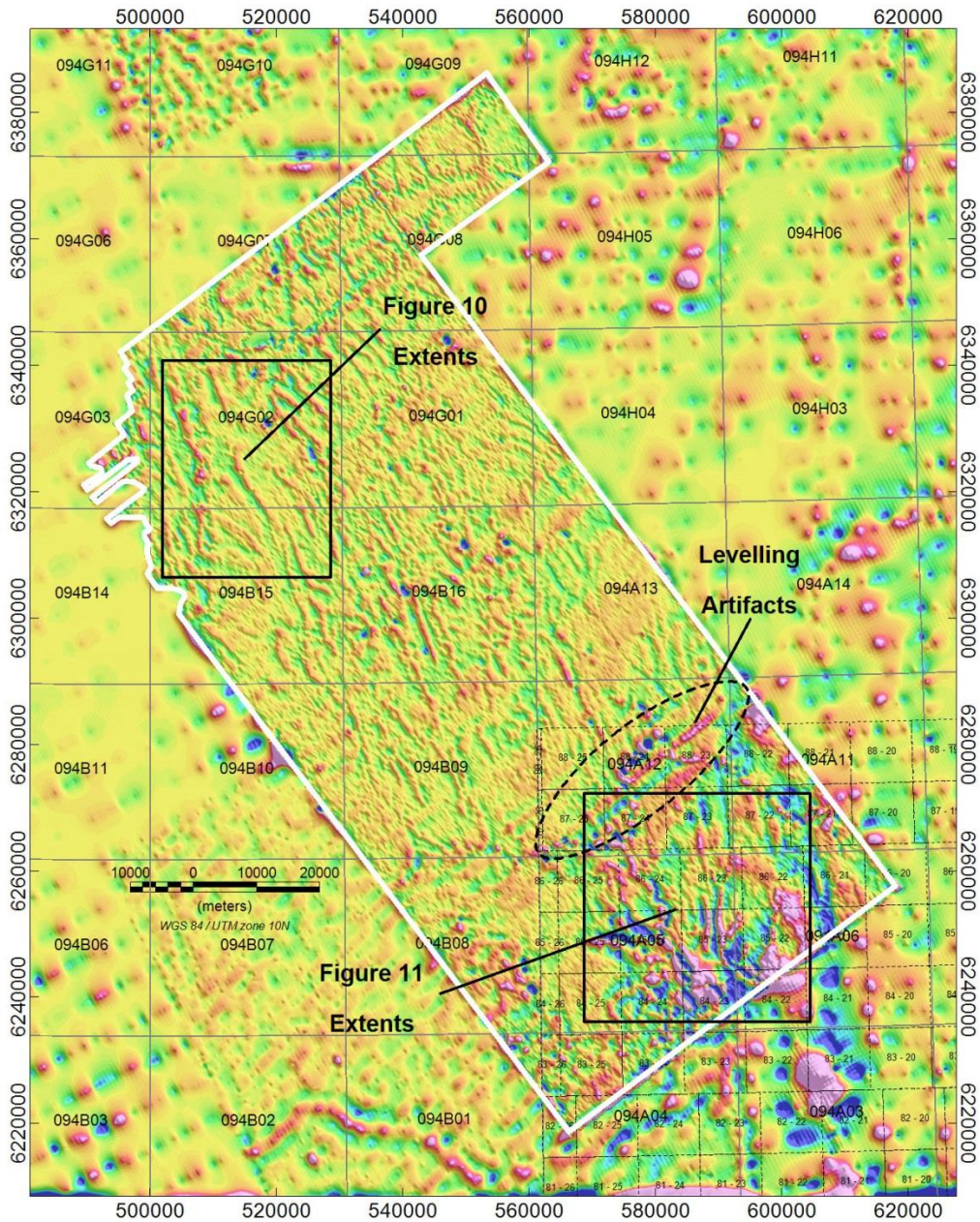


Figure 9 – Residual Magnetic Field Grid of Top 2000m.

There is also a magnetic fabric in the data that is closely aligned with the topography. The figure below shows data from the northwest area of the map. The image on the left shows the shallow magnetic component and some magnetic lineaments indicated. The image on the right shows the axes of the magnetic lineaments superimposed on SRTM topographic data.

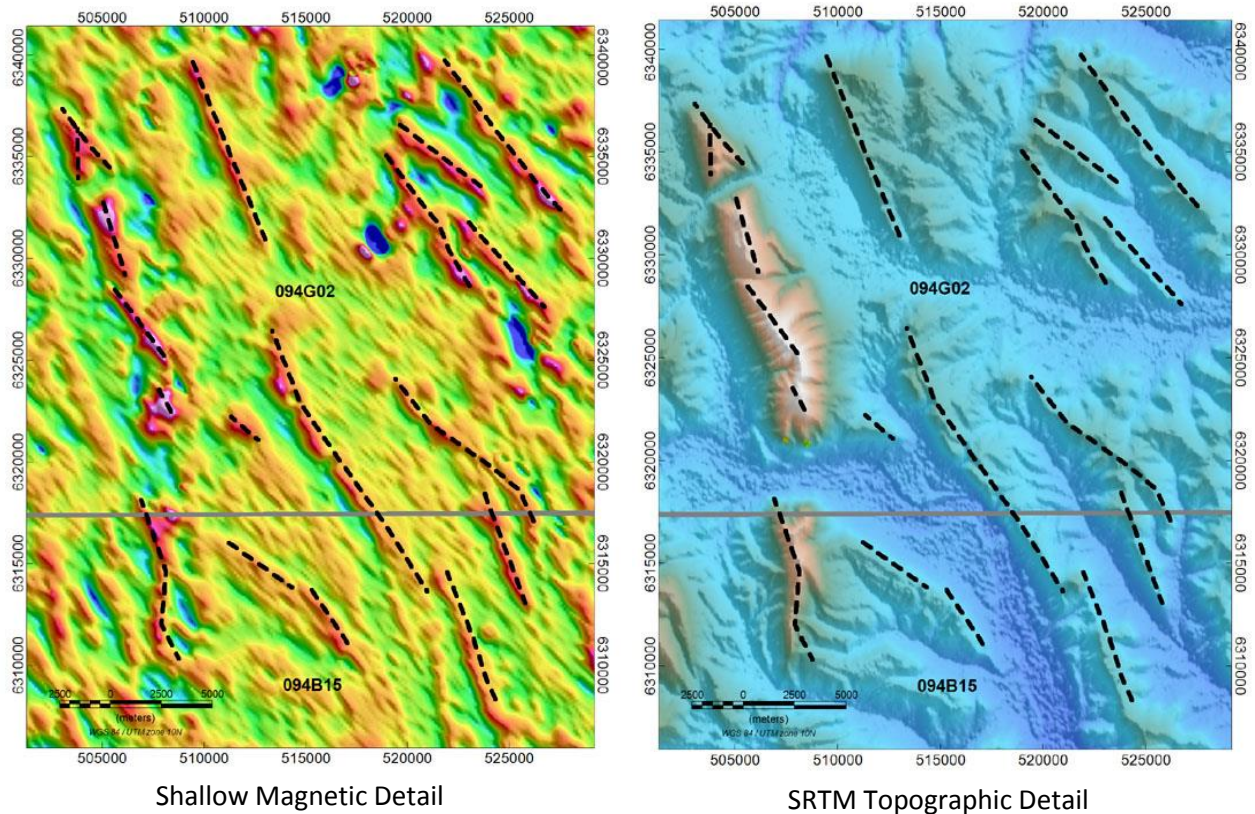


Figure 10 – Shallow Magnetic Fabric and Topographic Data

The close correlation between topographic ridges and magnetic highs, and valleys (drainage) and magnetic lows is apparent. This relationship is consistent with underlying rock with a measureable magnetic component. A magnetic low is associated with the relative absence magnetic source material over valleys and a relative increase when over ridges.

Towards the southern end of the area the pronounced ridge and valley character of the terrain lessens, possibly due to erosion or it is simply buried under added till cover. Figure 11a on the following page shows the shallow magnetic component grid, with drainage superimposed for an area in the southern end of the survey.

The drainage meanders without the stricter topographic control but the association of valleys with magnetic lows is generally still evident. Dashed outlines, noted with the letter 'H' indicate occasional areas where the relationship is reversed, and a magnetic high is associated with a topo low. A possible explanation is that the underlying rock, hosting an eroded river channel is less magnetic than river gravels accumulated in the channel.

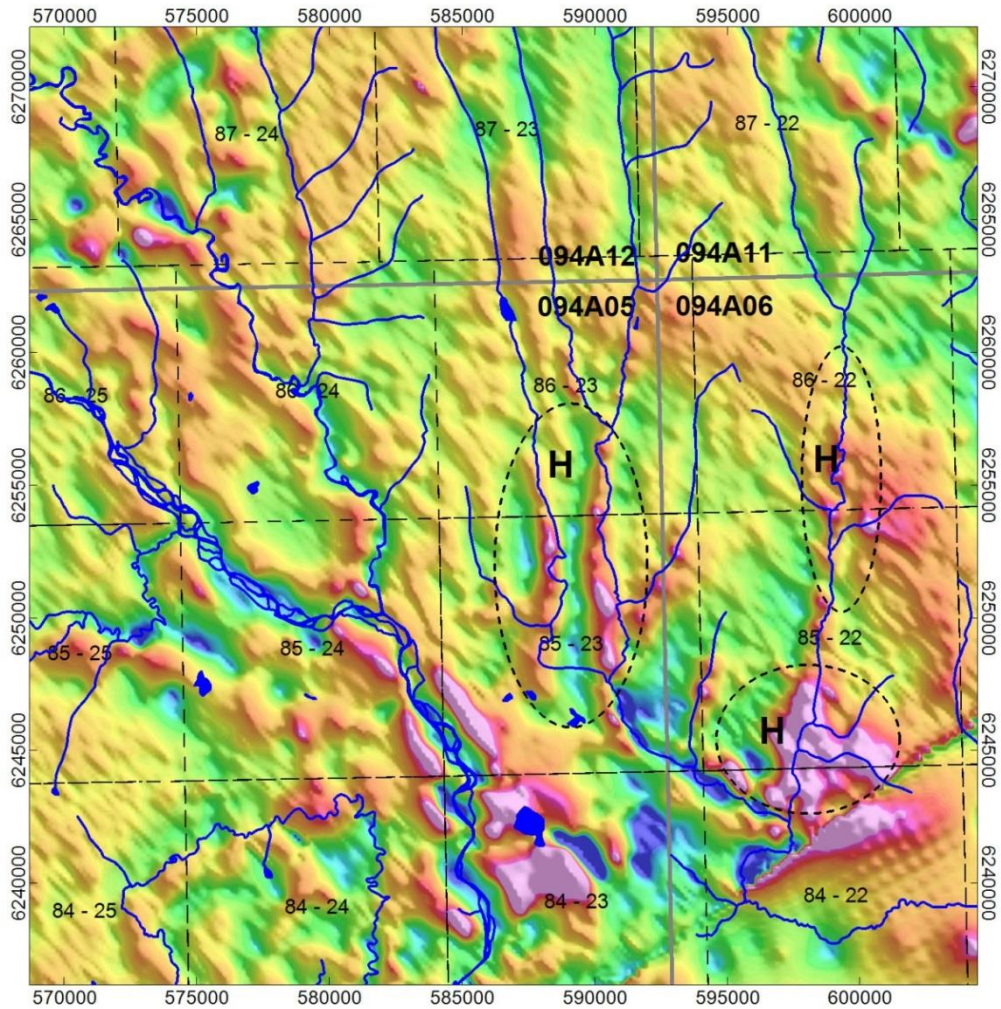
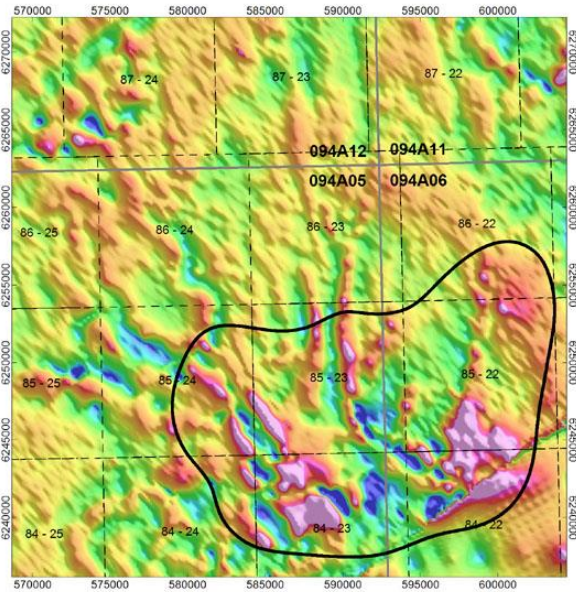


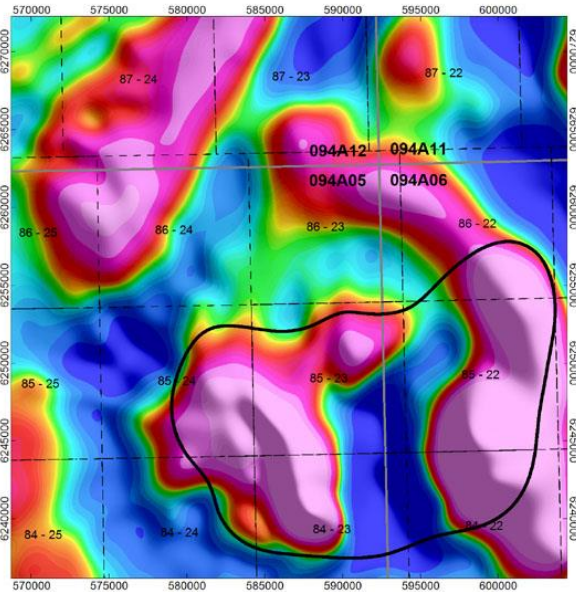
Figure 11a – Shallow Magnetic Fabric in the southern area of the survey

At the southeastern edge of the survey, there is increased magnetic signal in the shallow grid. This is a reflection of magnetic anomalies that are well defined in the 2km to 5 km depth slice. Figure 11b below shows data from the same area as Figure 11a on the previous page. The area of increased magnetic signal is noted. The shallow magnetic detail is shown on the left and the 2km to 5km depth slice grid is shown on the right.

This is a region where the underlying magnetic basement appears to be the shallowest and this is reflected as signal leakage in this overlying layer.



Shallow Magnetic RMI



2km to 5 km Layer RMI

Figure 11b – Shallow Magnetic Fabric and 2 to 5 km Layer RMI

## 4.4. Calculated Vertical and Horizontal Derivatives

The calculated vertical magnetic derivative sharpens the magnetic signature from relatively shallow sources and attenuates the signature from deeper sources including regional gradients. The horizontal width of the vertical gradient anomaly is about one half of that of the total field anomaly. This enhancement of anomalies associated with near surface sources resolves detail that may not be evident in the total field presentation. If the width of the magnetic source is significant, greater than the sensor height above the source, the zero contour of the vertical gradient reflects the location of the magnetic contact.

Fourier filters were used to calculate first and second vertical derivative grids for the pole-reduced total magnetic field grid, as well as each of the four depth slice grids.

The horizontal magnetic gradient highlights geological contacts (where the horizontal is at a maximum). The horizontal gradient ( $G_{hor}$ ) is simply the vector sum of the gradients in the East ( $G_E$ ) and North ( $G_N$ ) directions:

$$G_{hor} = \sqrt{G_E^2 + G_N^2}$$

Horizontal gradient grids were calculated for the pole-reduced total magnetic field grid, as well as each of the four depth slice grids.

## 4.5. Apparent Magnetic Susceptibility

The apparent magnetic susceptibility process assumes that the ground beneath the survey can be represented by a grid of vertical rectangular prisms, each with a surface dimension of the grid cell size of the magnetic field grid. The process calculates the susceptibility for each prism that would reconstitute the measured total magnetic field.

If the actual magnetic formations are deeper than assumed, or do not have significant depth extent, the true susceptibility will be underestimated. Nevertheless, the process does recognize that smaller magnetic sources require a higher susceptibility to produce the same anomaly amplitude as a larger source with lower susceptibility. The resolution at best cannot be finer than the cell size of the magnetic grid. A narrower, more concentrated magnetic source will not be assigned its true susceptibility but be attributed to a larger prism volume of lower susceptibility that would produce the same net effect.

Magnetic susceptibility grids were calculated for the pole-reduced TMI grid, as well as for each of the four depth-slice grids.

## 4.6. Three Dimensional Magnetic Inversion

The magnetic data was inverted using the program *MAG3D*, developed by the Geophysical Inversion Facility of the Department of Geophysics and Astronomy at the University of British Columbia (UBC-GIF). The program derives magnetic susceptibility values for a 3D voxel mesh below the magnetic survey datum. The computed array of magnetic susceptibility voxels, when combined, will produce the total magnetic field grid.

The inversion routine is very processing-intensive and had to be carried out over four separate runs for four overlapping data selections. The four inversion solutions were merged together for the final presentation. The voxel dimensions were 400m x 400m horizontally. The vertical size of the voxels started at 100m at the surface and gradually increased with depth. The figure below shows a perspective view of the complete voxel array mesh, looking north.

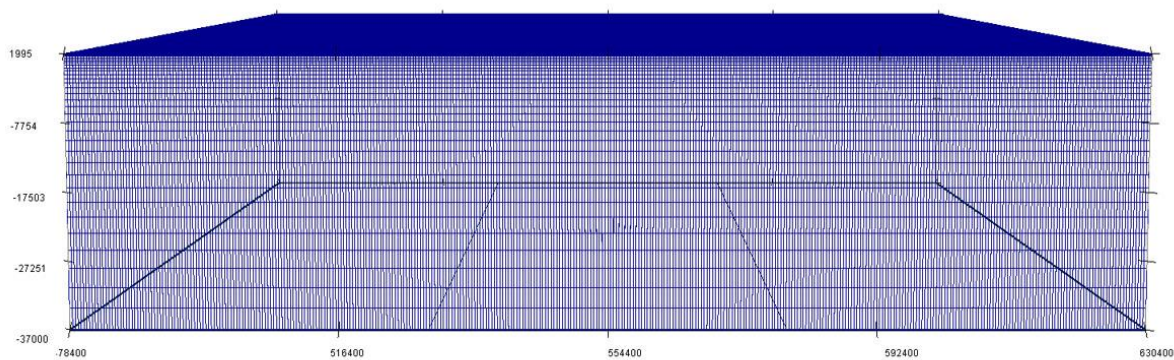


Figure 12 – Inversion Voxel Array – South End looking North

The magnetic inversion data is included with this report in a variety of formats, as well as viewing software and Internet links to download viewing software. A number of vertical susceptibility section grids (Geosoft format) have been generated at regular intervals in the north-south direction.

As an illustration of the flexibility of the software, the image below shows a view of the 3D voxel array, together with selected vertical sections, from Geosoft's OASIS montaj viewer. The view is looking north-east and the 3D array has been cut into from the west and top.

The vertical dimension of the inversion array is elevation above sea level.

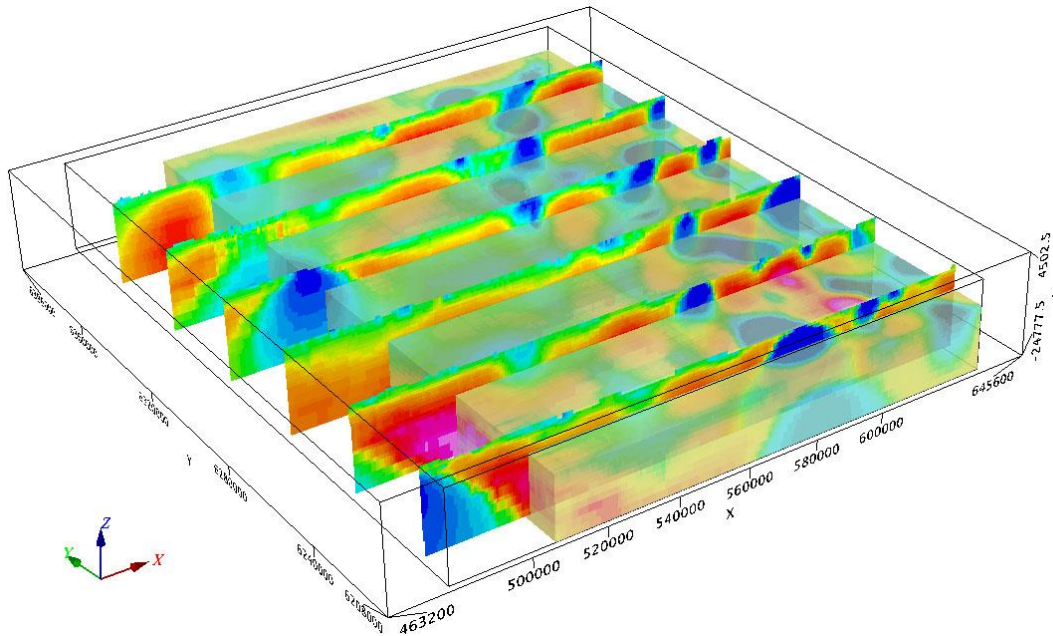


Figure 13 – 3D Inversion Susceptibility Voxel with Selected Vertical Sections

It is important to note that the inversion solution is not unique. There are an infinite number of potential magnetic susceptibility distributions in the voxel array that would produce the input data. The solution derived in the inversion process is but one of those solutions. The results need to be examined carefully, with consideration of the input data.

## **4.7. Multi-Mod Magnetic Models**

To compliment the inversion solution of the Mag3D process, a number of magnetic anomalies were inverted using the program Multi-Mod. The program, developed by Scott Hogg & Associates Ltd., utilizes a simple enclosed dipping tabular body of uniform susceptibility. This allows for sharp susceptibility contrasts, as opposed to the gradual transitions presented by Mag3D.

The tabular form has horizontal upper and lower surfaces and parallel dipping sides. The depth, width (horizontal), thickness (vertical), dip and susceptibility are variable parameters that can be adjusted to optimize the least squares fit to the observed magnetic profile.

Magnetic anomalies are additive. Each magnetic source has its own magnetic signature and when two sources are located near each other, horizontally or vertically, the resultant magnetic anomaly is simply the sum of the individual anomalies. Inaccuracy and uncertainty of model result arise as the anomalous response from the individual bodies overlap and cannot be unambiguously separated from each other. Multi-Mod allows for up to 5 bodies to be simultaneously considered. The parameters for all bodies can be optimized as a single fit to minimize the difference between the combined magnetic response and the observed magnetic profile.

The survey profile data was not amenable to the modelling process, as so many of the flight lines were flown in segments. It was very unusual to find a single flight line that adequately captured an anomaly. To obtain a set of suitable magnetic profiles, lines were digitized across the features of interest and profile data was extracted from the TMI compilation grid. This approach also allowed for the inclusion of regional anomalies outside the survey area.

A report, like the sample shown below is included for each model in an appendix to this report and all the model results are summarized in a table on the following page. A column indicating the model body elevation above sea level has been added to the summary table, for comparison with the inversion results.

The residual magnetic field image in the lower right shows the individual bodies in plan view, with the flight line chosen for the model shown as a heavy black line. The image in the lower left shows the same bodies in section view. The horizontal dashed line represents the surface. Individual profile responses are shown above as colour-coded dashed lines. The aggregate of the individual responses is indicated by a solid red line and the measured magnetic profile is shown as a black line.

The table in the upper right summarizes the individual parameters.

- The depths listed in the model reports are below magnetic datum.
- All dimensions and coordinates are in metres
- Magnetic susceptibility is given in milli-emu SI units (e.g. 28.2 milli emu = 0.0282 emu)

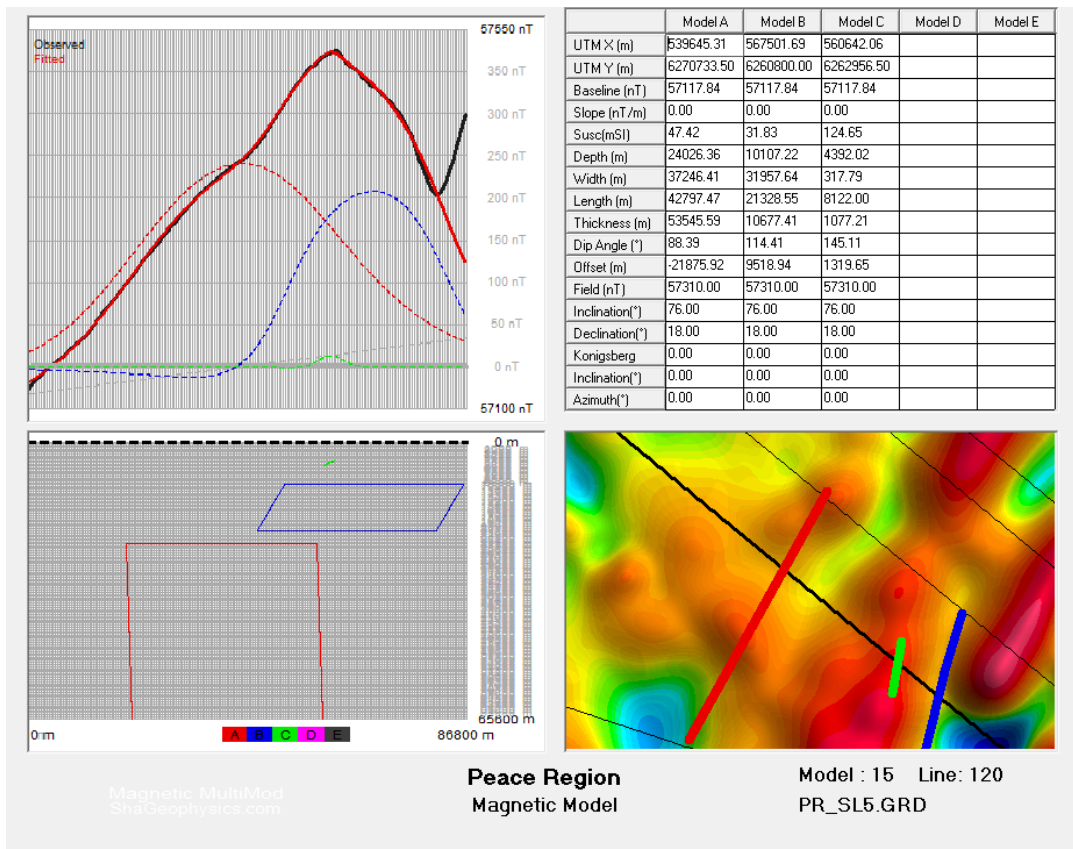


Figure 14 – Sample Model Report

The table below summarizes the model results.

Model	Body	Easting	Northing	Depth (sensor)	Elevation (sea level)	Width	Thickness	Dip	Susc (SI)	Length	Strike
1	A	580684	6304506	14,730	-13,823	1131	10000	130	0.81326	23219	38
2	A	573557	6296604	11,307	-10,452	1246	10000	117	0.33004	23219	38
3	A	555757	6242006	15,092	-14,209	37049	10000	149	0.08217	22559	24
3	B	556832	6241648	5707	-4850	1502	5000	158	0.15247	10594	25
4	B	512688	6239076	11,175	-9791	922	34000	137	0.79595	5752	22
4	C	527937	6232714	15,262	-13,594	2265	10492	99	0.62589	8923	29
5	A	586931	6244313	6727	-6019	577	150000	114	0.64198	7177	-23
5	B	599374	6244150	6571	-5874	523	11656	79	0.85132	15217	-6
7	A	594397	6227296	7022	-6295	1252	13490	59	0.27250	17989	-51
7	B	604895	6227218	5003	-4298	668	96931	67	0.70837	9870	-41
8	A	579783	6263926	4943	-4197	197	9022	149	0.49360	27709	28
9	A	624390	6370166	8321	-7486	2028	11018	139	0.21821	36418	39
10	A	570700	6364049	21,512	-20,544	6651	28737	75	0.78874	47489	39
10	B	540359	6364049	20,055	-19,070	5423	9511	70	0.50583	14943	-15
11	A	585171	6277294	7755	-6811	1367	17259	115	0.17178	27711	27
11	B	568108	6291306	12,559	-11,611	1563	20000	67	0.33704	23219	38
12	A	552912	6343179	17,530	-16,488	9455	9735	83	0.20344	47489	39
12	B	544071	6350440	15,377	-14,335	3152	12363	99	0.23584	14943	-15
13	A	542532	6215516	13,202	-12,493	3762	10000	22	0.30700	18024	4
14	A	606899	6343716	7852	-7048	1873	10000	145	0.23683	7125	13
14	B	615944	6338682	8468	-7672	6889	10000	116	0.03243	18973	-6
15	A	543578	6277791	24,026	-23,166	37246	53546	88	0.04742	42797	29
15	B	566971	6258580	10,107	-9356	31958	10677	114	0.03183	21329	13
15	C	560762	6263678	4392	-3662	318	1077	145	0.12465	8122	9
16	A	550995	6287566	5050	-4269	299	10000	105	0.10418	13559	58
17	A	553324	6379568	27,773	-26,791	5303	37944	123	0.90473	33493	-15
17	B	577451	6379568	18,754	-17,970	7640	5933	153	0.73677	16961	-33
18	A	616600	6243922	8708	-7849	609	10000	122	0.61810	14196	-16
18	B	601679	6244119	7357	-6550	908	10000	129	0.78049	15217	-6
19	A	613127	6301153	10,004	-9220	717	10000	77	0.70291	13938	-11

Table 1 – Magnetic Model Results

A graphic representation of the model results in plan view is shown below. The background image is the 5km to 15km depth slice RMI grid. The interpreted possible faults from Figure 8 are included.

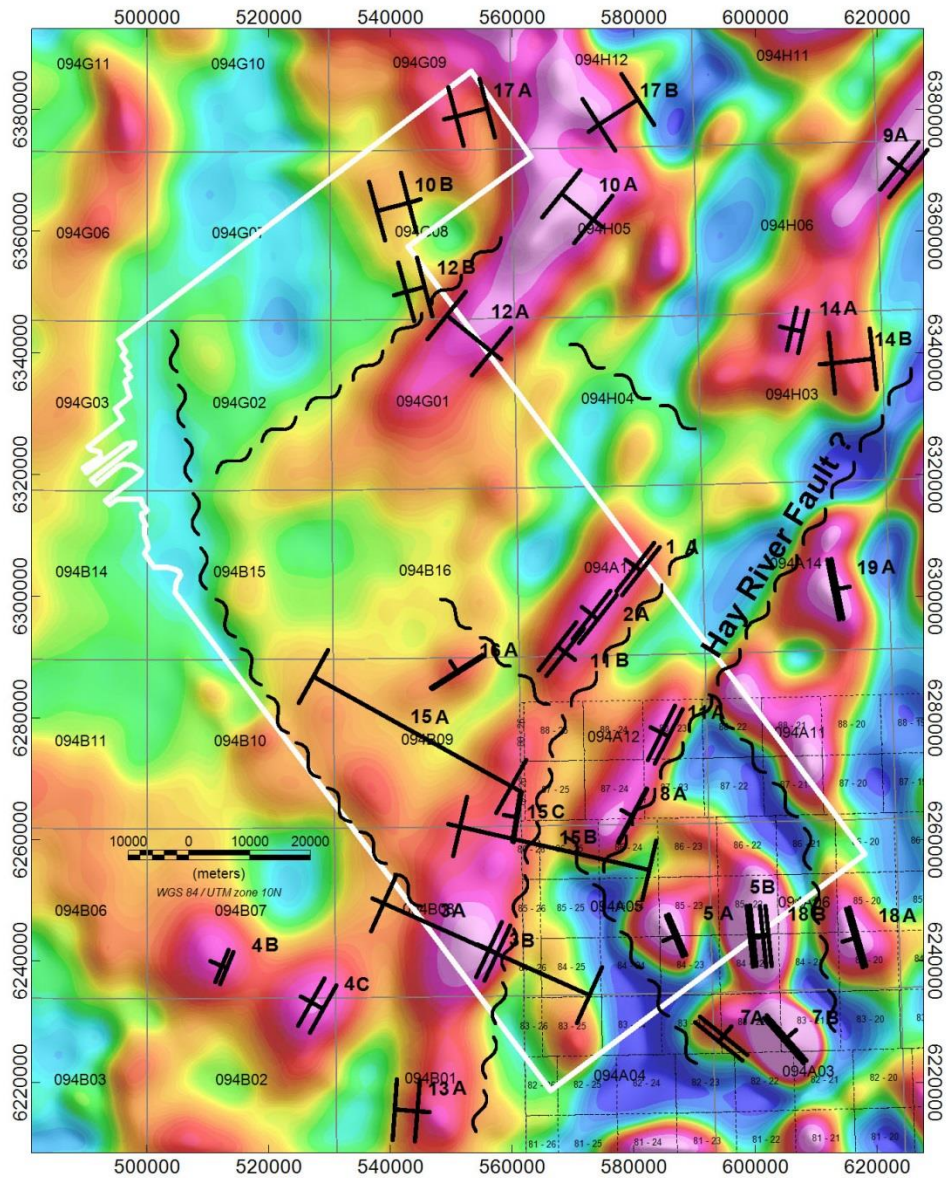


Figure 15a – Model Results on 5km to 15km Depth Slice RMI Grid

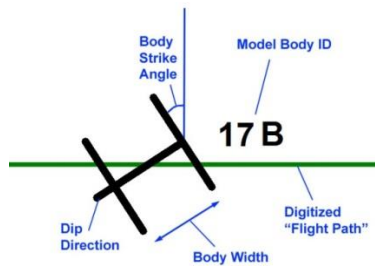


Figure 15b – Model Graphic Legend

## 5. Discussion

### 5.1.3D Inversion

The figure below includes two images. The bottom image shows a vertical magnetic susceptibility section at 6,318,000m North. The colour range is set between 0 and 0.02 SI emu units. The vertical scale is elevation relative to sea level. The image at the top shows the residual magnetic field grid of the depth slice 5km to 15km. The location of the section is shown with a grey line. The SkyTEM survey boundary is shown for reference as a white line.

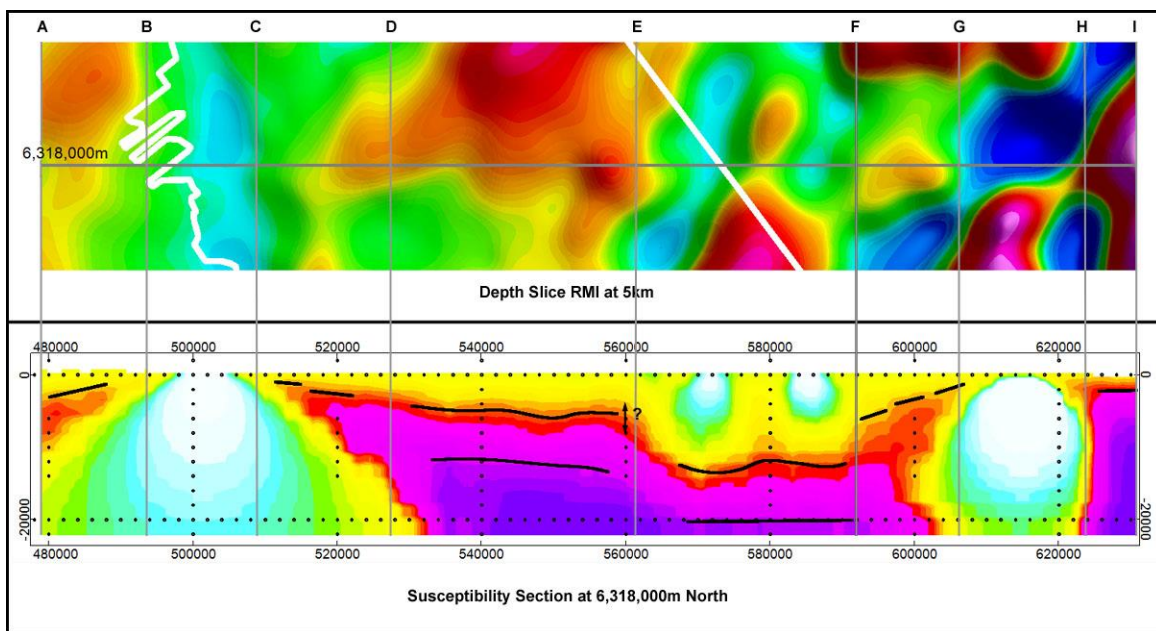


Figure 16 – Sample Susceptibility Section and RMI Grid

The above section was chosen for discussion because it illustrates some of the pitfalls of the inversion process, particularly in areas where there is an absence of magnetic material in the basement. The basement is overlain by sedimentary rock, which is expected to be virtually non-magnetic. It is therefore expected that a change of magnetic susceptibility would be evident where the basement begins.

This is generally what is observed in the area between reference points D and E, where the susceptibility colour transitions from yellow, quickly through orange to red. The depth of this transition, 3000m to 5000m below sea level, is consistent with the observations made in the FFT amplitude spectrum analysis (sec 4.3). A horizontal line has been drawn, but its vertical position at this point is a little uncertain.

The magnetic susceptibility is observed to generally increase with depth. A second horizontal line has been drawn at a second instance of susceptibility change. This occurs at a depth of approximately 15km below sea level and could be an indication of the very deep sub-basement layer examined in section 4.3.

Between E and F are two magnetic lows. The inversion algorithm's solution was to plunge the contact interpreted in DE to great depth. In BC and GH, larger magnetic lows are evident and the corresponding susceptibility solution is null. In the zones, between the magnetic rock and the non-magnetic rock (AB, CD, FG and HI), the susceptibility contrast becomes shallower. This apparent rise of the basement is not considered to reflect the actual depth. It is possibly a solution to accommodate the abrupt fall-off of magnetic field at the contact zones.

### Depth to Shallow Basement

Where there is sufficiently magnetic material in the basement, the 3D inversion has produced a workable solution and a horizontal layer of magnetic material has been observed beneath a section that is virtually non-magnetic, indicating the shallow basement. In areas where the basement rock is particularly non-magnetic, the inversion solution does not appear to reflect a reliable depth. A threshold susceptibility value of 0.003 emu was chosen to represent the point in the inversion data where the basement begins. The inversion data was examined and the elevation where this susceptibility change occurred was extracted. These elevations were masked against the source data and regions of little magnetic activity were excluded. The result was gridded, using a minimum curvature algorithm.

Figure 17 on the following page shows the elevation grid, with the SkyTEM survey boundary included for reference. Interpreted possible faults from Figure 8 are included for reference.

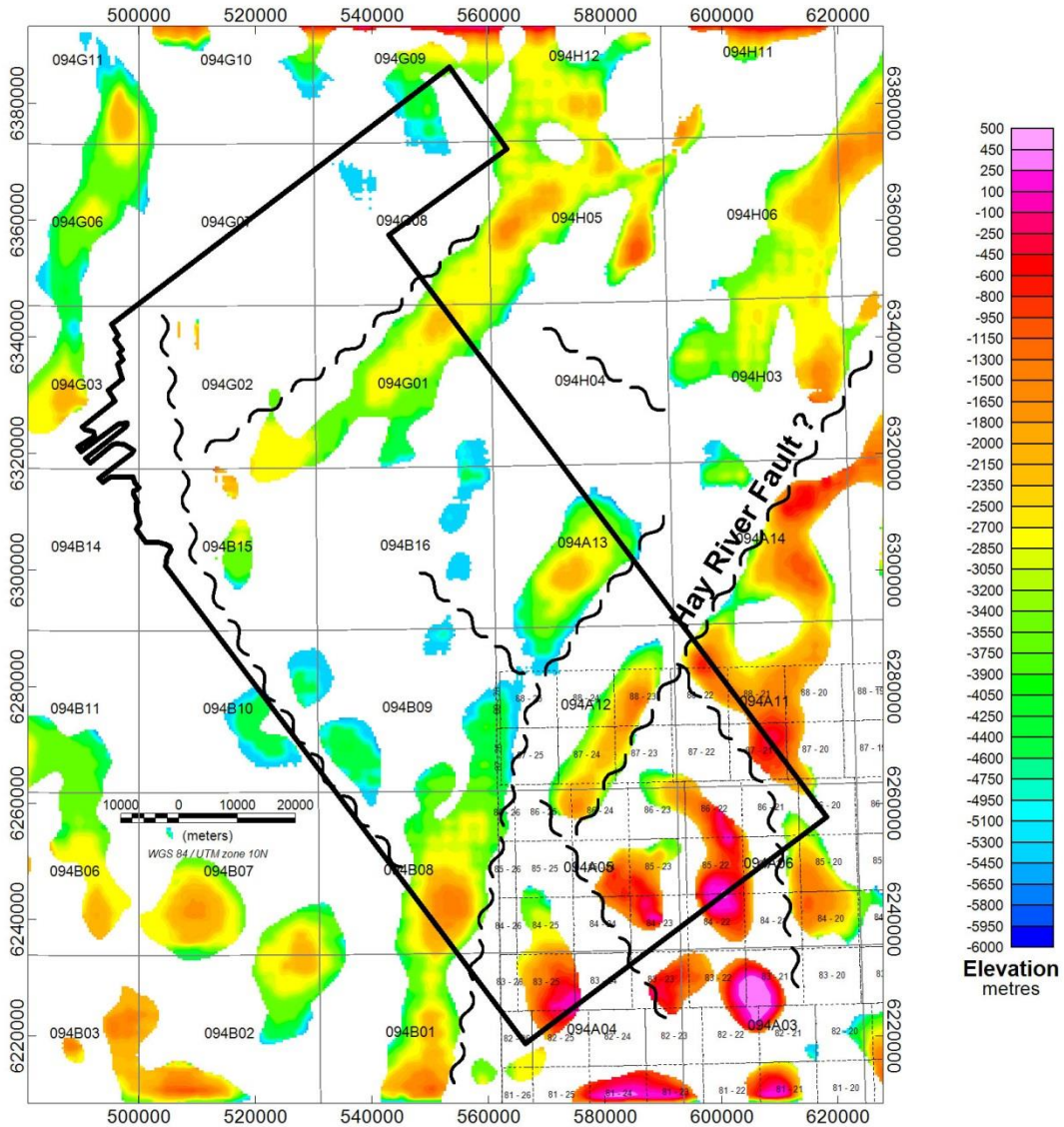


Figure 17 – Elevation of Shallowest Magnetic Layer

At the elevation of the interpreted basement transition zone, the vertical dimension of the inversion voxels was 600m to 700m. With such coarse resolution, the above grid can only be used as a very general reference. In general, the layer appears to originate at elevations between 2000m and 5000m below sea level. This is roughly in line with the depth slice layer (sec 4.3) that suggested magnetic material originating at a depth 5000m below magnetic sensor (the survey altitude varied between 600m and 2000m above sea level).

According to the inversion data, the elevation in the southeast portion of the map is significantly higher than the rest of the area, indicating that the basement is shallower in the southeast. This may be due to an up thrust in the southeast along the Hay River fault, or may be a reflection of the Peace River Arch, or a combination of the two.

To investigate the deeper susceptibility transition observed in Figure 16, a higher susceptibility threshold of 0.0125 emu was chosen and the elevations of this transition were extracted. Again, the results were masked against the magnetic field data and areas of little magnetic activity were excluded.

Figure 18 below shows the elevation grid, along with the survey area and possible faults for reference.

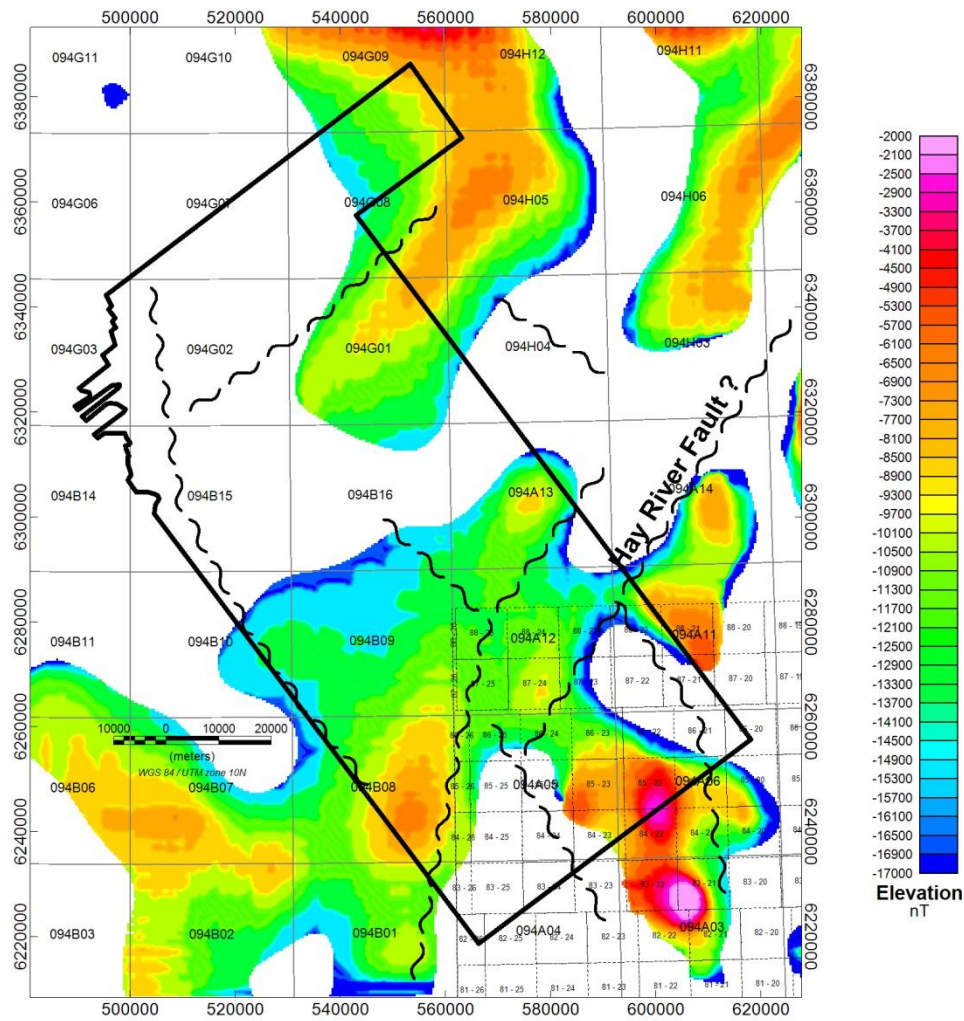


Figure 18 – Elevation Grid of Deep Susceptibility Transition

In general, the elevation of this layer is bound between 7000m and 15000m below sea level. Deeper portions can be observed at the edges of the useable part of the data, but the reliability of the depth solution become suspect (as shown in Figure 16). As with the shallow layer, there appears to be an rising or up-thrust of the deep layer in the southeast portion of the map.

## 5.2. Magnetic Model Results

The depths reported in the magnetic models were converted to elevation below sea level, for comparison with the inversion results. The model bodies have been plotted in Figure 19 below, with their elevations below sea level plotted as negative values. The colour background shows the deep susceptibility interface. Possible basement faults are included for reference.

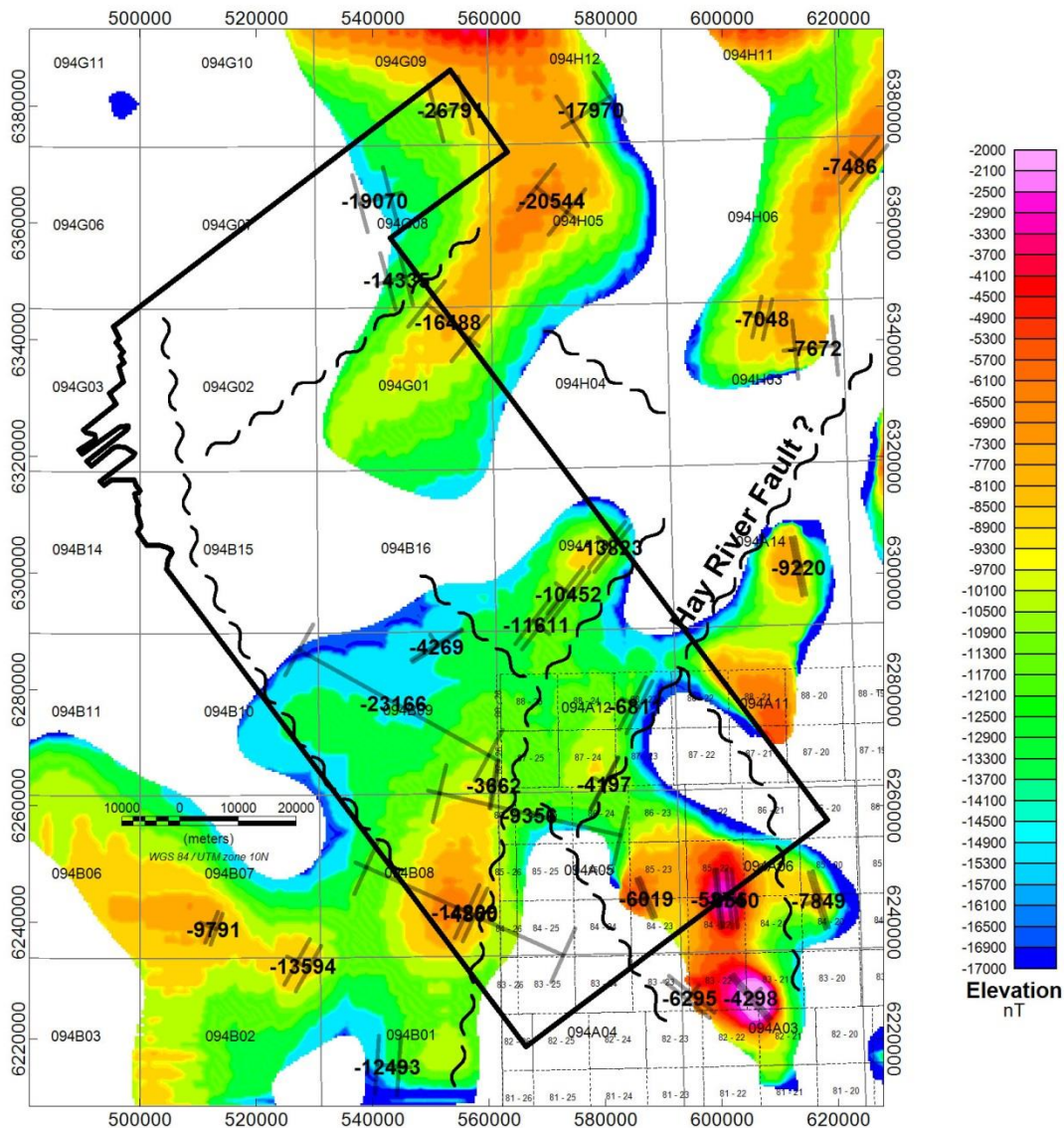


Figure 19 – Magnetic Model Elevation Results on Deep Basement Layer

In general, the depths implied by the magnetic models are in closer agreement with the deeper interface map of the 3D inversion. The shallowest depths in the range of 4000m to 6000m below sea level occur in the southeastern corner. The most notable difference is the northwestern sector, where

the group of models suggests a depth in the range of 15,000m to 20,000m below sea level. The modelled bodies are predominantly steeply dipping and are well delineated by the depth slice maps at 5000m and 15,000m.depth.

Respectfully submitted,

---

Steve Munro  
Chief Geophysicist  
Scott Hogg & Associates Ltd.  
Toronto, Canada  
September 29, 2016

---

R.L. Scott Hogg, P.Eng.  
President  
Scott Hogg & Associates Ltd.  
Toronto, Canada  
September 29, 2016

# Appendix I – Digital Products Summary

## Grids

The following Geosoft format grids have been included with this report.

### Pole-Reduced Magnetic Field

- Peace Pole-Reduced TMI
- Peace Depth Slice (top 2km) Pole-Reduced RMI
- Peace Depth Slice (2km to 5km) Pole-Reduced RMI
- Peace Depth Slice (5km to 15km) Pole-Reduced RMI
- Peace Depth Slice (15km plus) Pole-Reduced RMI

### Apparent Magnetic Susceptibility

- Peace Apparent Susceptibility
- Peace Depth Slice (top 2km) Apparent Susceptibility
- Peace Depth Slice (2km to 5km) Apparent Susceptibility
- Peace Depth Slice (5km to 15km) Apparent Susceptibility
- Peace Depth Slice (15km plus) Apparent Susceptibility

### Calculated Pole-Reduced Vertical Gradient

- Peace Pole-Reduced CVG
- Peace Depth Slice (top 2km) Pole-Reduced CVG
- Peace Depth Slice (2km to 5km) Pole-Reduced CVG
- Peace Depth Slice (5km to 15km) Pole-Reduced CVG
- Peace Depth Slice (15km plus) Pole-Reduced CVG

### Calculated Pole-Reduced 2<sup>nd</sup> Vertical Gradient

- Peace Pole-Reduced 2VG
- Peace Depth Slice (top 2km) Pole-Reduced 2VG
- Peace Depth Slice (2km to 5km) Pole-Reduced 2VG
- Peace Depth Slice (5km to 15km) Pole-Reduced 2VG
- Peace Depth Slice (15km plus) Pole-Reduced 2VG

### Pole-Reduced Calculated Horizontal Gradient

- Peace Pole-Reduced HGrad
- Peace Depth Slice (top 2km) Pole-Reduced HGrad
- Peace Depth Slice (2km to 5km) Pole-Reduced HGrad
- Peace Depth Slice (5km to 15km) Pole-Reduced HGrad
- Peace Depth Slice (15km plus) Pole-Reduced HGrad

## Maps

The following Geosoft format maps have been included with this report.

- Peace Region Basemap
- Peace Region Pole-Reduced TMI
- Peace Region Depth Slice (top 2km) Pole-Reduced RMI
- Peace Region Depth Slice (2km to 5km) Pole-Reduced RMI
- Peace Region Depth Slice (5km to 15km) Pole-Reduced RMI
- Peace Region Depth Slice (15km plus) Pole-Reduced RMI

## Images

The following have been provided in JPEG, PDF and GeoTIFF format.

- Peace Region Pole-Reduced TMI
- Peace Region Depth Slice (top 2km) Pole-Reduced RMI
- Peace Region Depth Slice (2km to 5km) Pole-Reduced RMI
- Peace Region Depth Slice (5km to 15km) Pole-Reduced RMI
- Peace Region Depth Slice (15km plus) Pole-Reduced RMI

## 3D Inversion Files

Inversion data has been included in three formats

### Geosoft

- Geosoft format 3D Susceptibility voxel array file
- Geosoft format 3D map
- Geosoft format grids of vertical magnetic susceptibility sections at two km north-south intervals

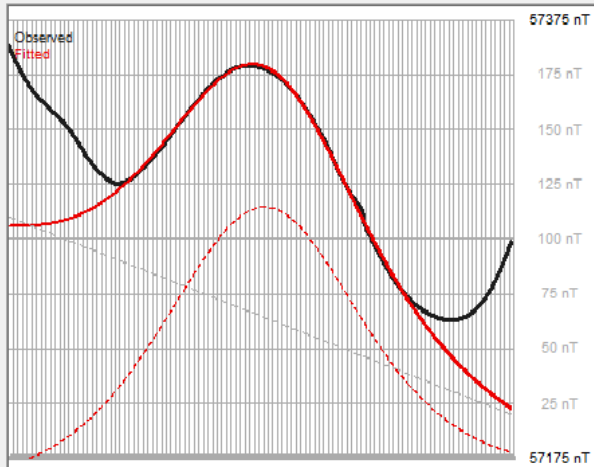
### UBC

- UBC format mesh and susceptibility files
- Meshtools3D – Viewing software
- PDF Section File - Vertical magnetic susceptibility sections at two km north-south intervals

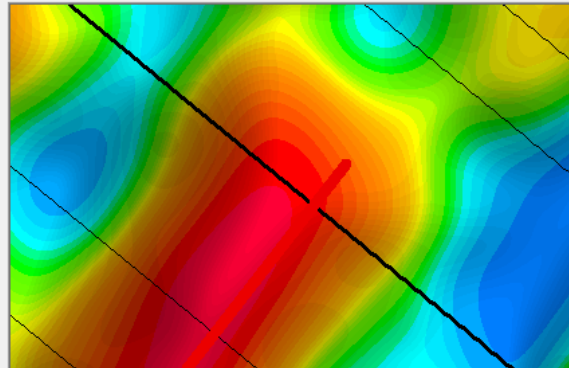
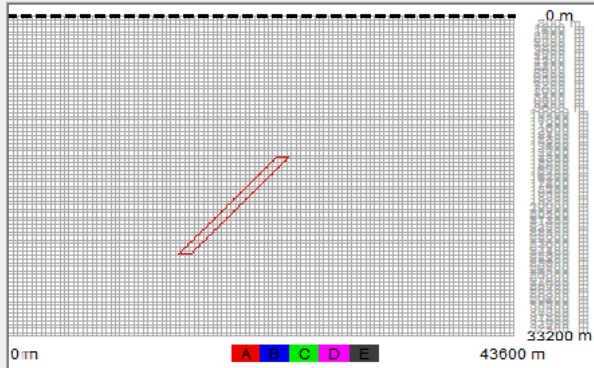
### ASCII

- ASCII format file of susceptibility array (easting, northing, elevation, susceptibility)

## **Appendix II – Model Report Pages**



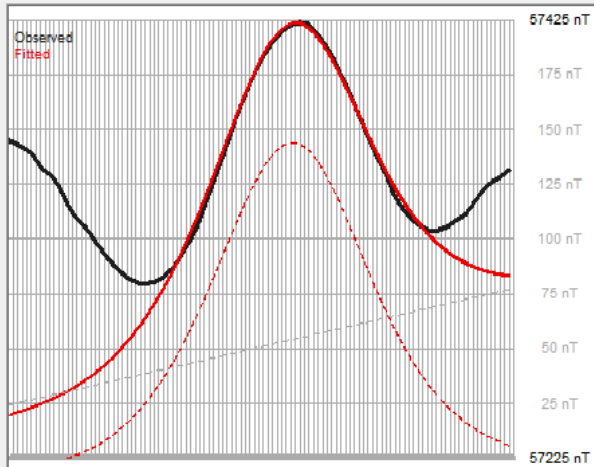
	Model A	Model B	Model C	Model D	Model E
UTM X (m)	575668.44				
UTM Y (m)	6298049.00				
Baseline (nT)	57284.68				
Slope (nT/m)	0.00				
Susc(mSI)	813.26				
Depth (m)	14730.49				
Width (m)	1130.94				
Length (m)	23218.80				
Thickness (m)	10000.00				
Dip Angle (°)	130.14				
Offset (m)	2103.58				
Field (nT)	57310.00				
Inclination(°)	76.00				
Declination(°)	18.00				
Konigsberg	0.00				
Inclination(°)	0.00				
Azimuth(°)	0.00				



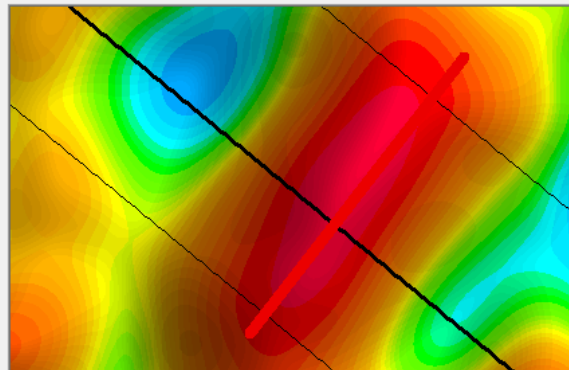
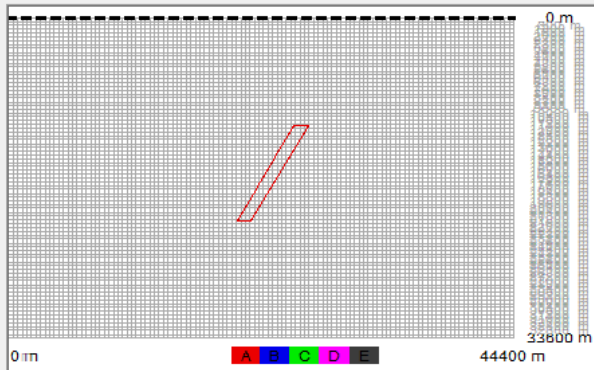
Magnetic MultiMod  
ShaGeophysics.com

**Peace Region**  
Magnetic Model

Model : 1 Line: 80  
PR\_SL5.GRD



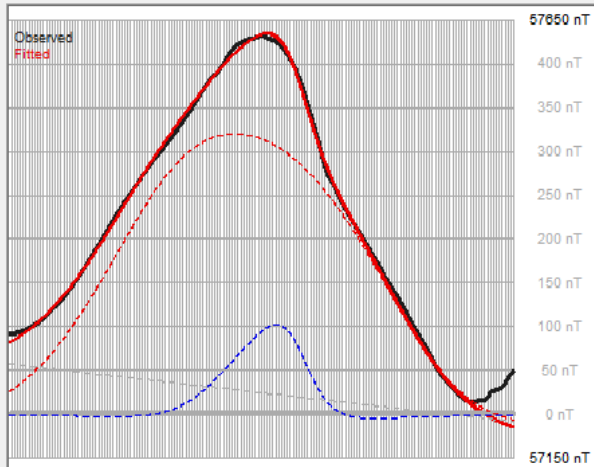
	Model A	Model B	Model C	Model D	Model E
UTM X (m)	575064.88				
UTM Y (m)	6298544.50				
Baseline (nT)	57249.19				
Slope (nT/m)	0.00				
Susc(mSI)	330.04				
Depth (m)	11307.10				
Width (m)	1245.96				
Length (m)	23218.80				
Thickness (m)	10000.00				
Dip Angle (°)	116.51				
Offset (m)	1322.65				
Field (nT)	57310.00				
Inclination(°)	76.00				
Declination(°)	18.00				
Konigsberg	0.00				
Inclination(°)	0.00				
Azimuth(°)	0.00				



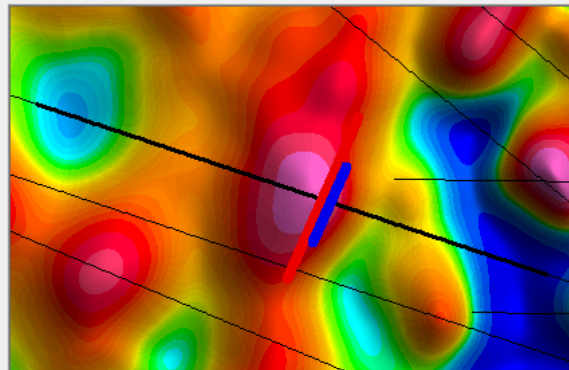
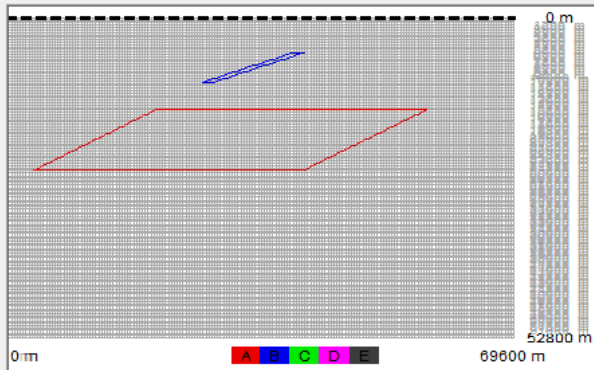
Magnetic MultiMod  
ShaGeophysics.com

**Peace Region**  
Magnetic Model

Model : 2 Line: 130  
PR\_SL5.GRD



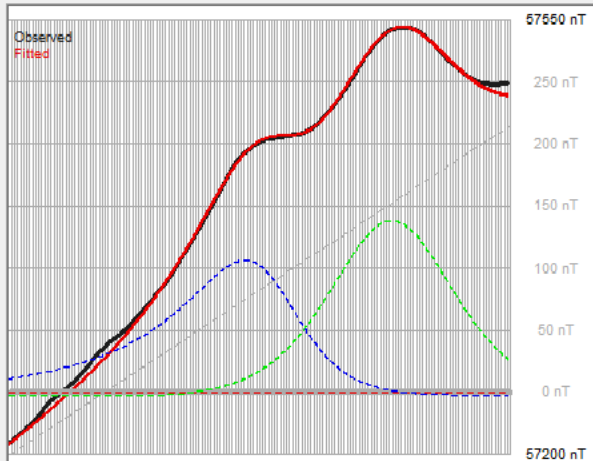
	Model A	Model B	Model C	Model D	Model E
UTM X (m)	555838.75	556702.50			
UTM Y (m)	6242192.50	6241370.00			
Baseline (nT)	57256.85	57256.85			
Slope (nT/m)	0.00	0.00			
Susc(mSI)	82.17	152.47			
Depth (m)	15091.58	5706.58			
Width (m)	37049.37	1501.79			
Length (m)	22559.32	10594.28			
Thickness (m)	10000.00	5000.00			
Dip Angle (°)	149.19	158.20			
Offset (m)	4362.78	4147.33			
Field (nT)	57310.00	57310.00			
Inclination(°)	76.00	76.00			
Declination(°)	18.00	18.00			
Konigsberg	0.00	0.00			
Inclination(°)	0.00	0.00			
Azimuth(°)	0.00	0.00			



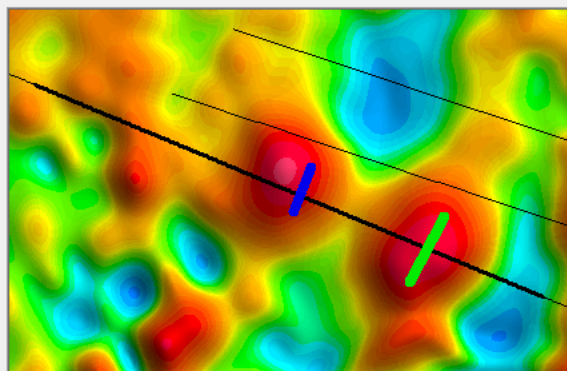
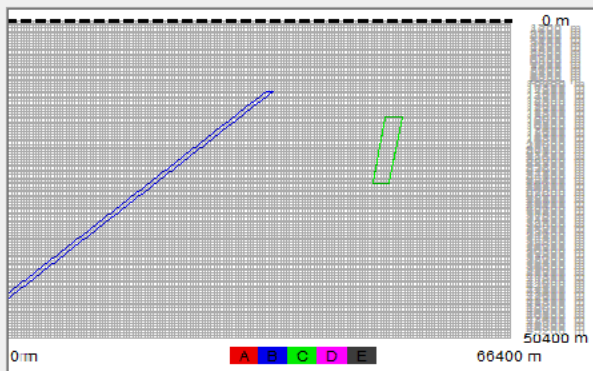
Magnetic MultiMod  
ShaGeophysics.com

**Peace Region**  
Magnetic Model

Model : 3 Line: 20  
PR\_SL5.GRD



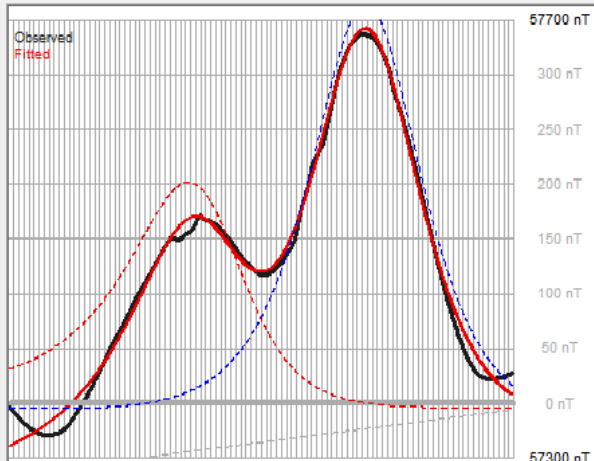
	Model A	Model B	Model C	Model D	Model E
UTM X (m)		512972.94	527902.19		
UTM Y (m)		6239789.00	6232650.50		
Baseline (nT)		57199.26	57199.26		
Slope (nT/m)		0.00	0.00		
Susc(mSI)		795.95	625.89		
Depth (m)		11175.16	15262.01		
Width (m)		922.12	2265.04		
Length (m)		5751.96	8923.01		
Thickness (m)		33999.89	10492.24		
Dip Angle (°)		136.87	99.31		
Offset (m)		2888.05	159.90		
Field (nT)		57310.00	57310.00		
Inclination(°)		76.00	76.00		
Declination(°)		18.00	18.00		
Konigsberg		0.00	0.00		
Inclination(°)		0.00	0.00		
Azimuth(°)		0.00	0.00		



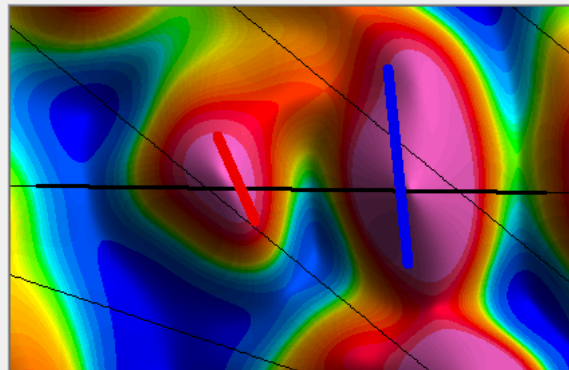
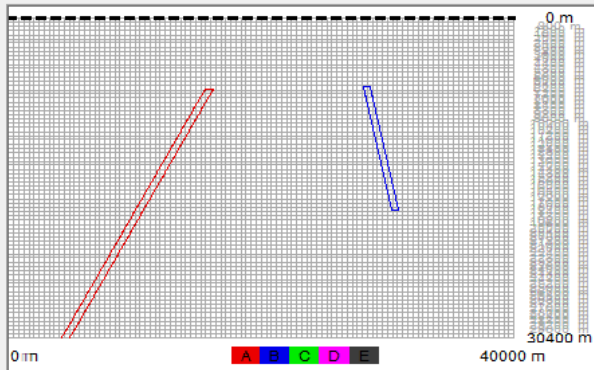
Magnetic MultiMod  
ShaGeophysics.com

**Peace Region**  
Magnetic Model

Model : 4 Line: 140  
PRVG\_SL5.GRD



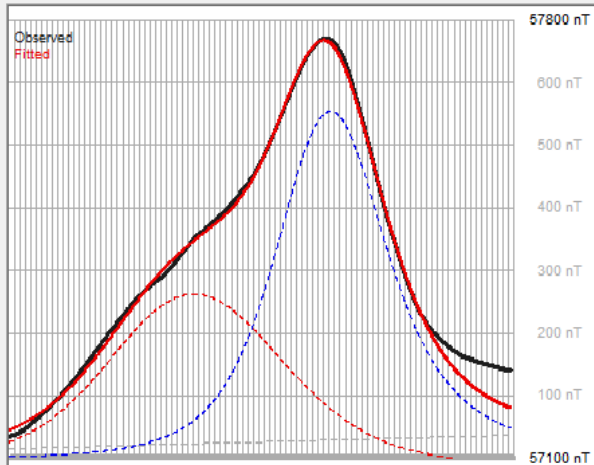
	Model A	Model B	Model C	Model D	Model E
UTM X (m)	586603.62	599178.94			
UTM Y (m)	6245069.50	6245992.00			
Baseline (nT)	57284.09	57284.09			
Slope (nT/m)	0.00	0.00			
Susc(mSI)	641.98	851.32			
Depth (m)	6727.34	6570.72			
Width (m)	576.62	523.14			
Length (m)	7176.53	15217.09			
Thickness (m)	150000.00	11656.01			
Dip Angle (°)	113.68	79.23			
Offset (m)	1167.00	-1301.52			
Field (nT)	57310.00	57310.00			
Inclination(°)	76.00	76.00			
Declination(°)	18.00	18.00			
Konigsberg	0.00	0.00			
Inclination(°)	0.00	0.00			
Azimuth(°)	0.00	0.00			



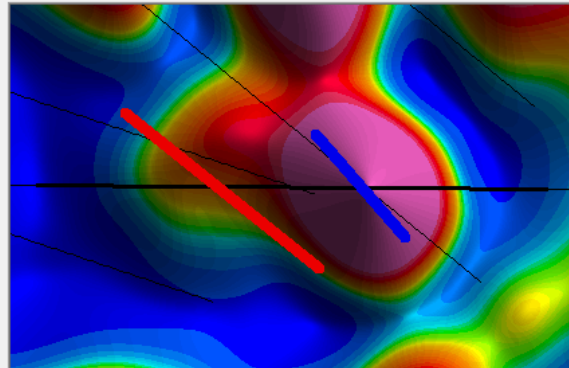
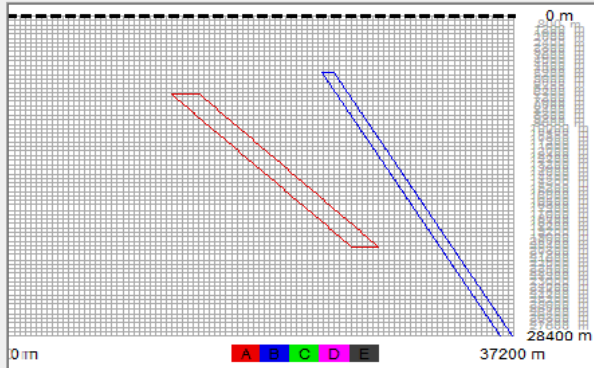
Magnetic MultiMod  
ShaGeophysics.com

Peace Region  
Magnetic Model

Model : 5 Line: 180  
PR\_SL5.GRD



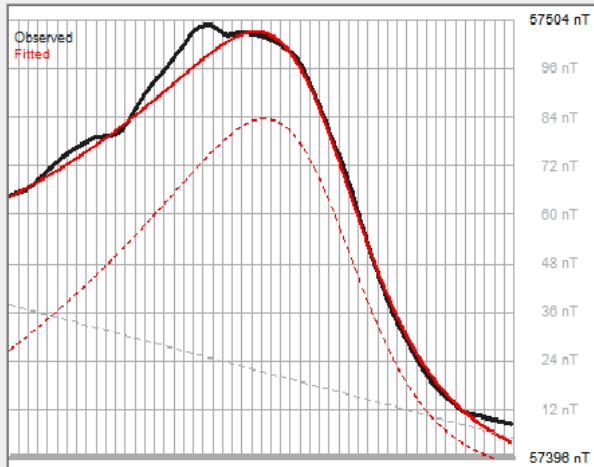
	Model A	Model B	Model C	Model D	Model E
UTM X (m)	594787.88	604767.25			
UTM Y (m)	6226985.00	6227363.00			
Baseline (nT)	57115.98	57115.98			
Slope (nT/m)	0.00	0.00			
Susc(mSI)	272.50	708.37			
Depth (m)	7022.20	5003.43			
Width (m)	1251.67	667.51			
Length (m)	17988.77	9870.22			
Thickness (m)	13490.25	96931.48			
Dip Angle (°)	58.89	67.21			
Offset (m)	-7829.07	-223.33			
Field (nT)	57310.00	57310.00			
Inclination(°)	76.00	76.00			
Declination(°)	18.00	18.00			
Konigsberg	0.00	0.00			
Inclination(°)	0.00	0.00			
Azimuth(°)	0.00	0.00			



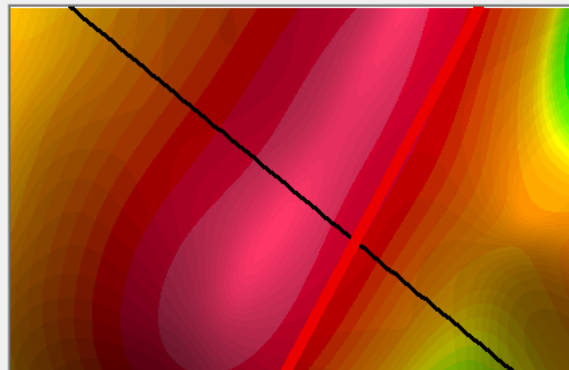
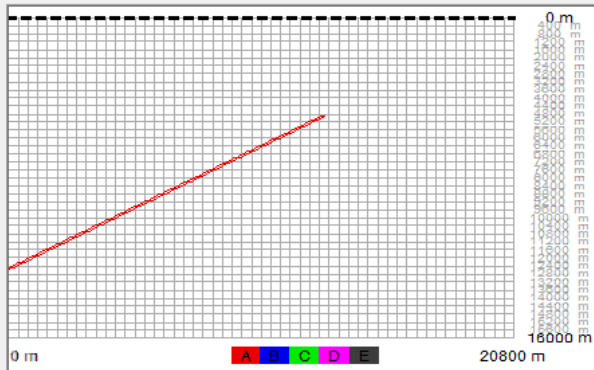
Magnetic MultiMod  
ShaGeophysics.com

**Peace Region**  
Magnetic Model

Model : 7 Line: 170  
PR\_SL5.GRD



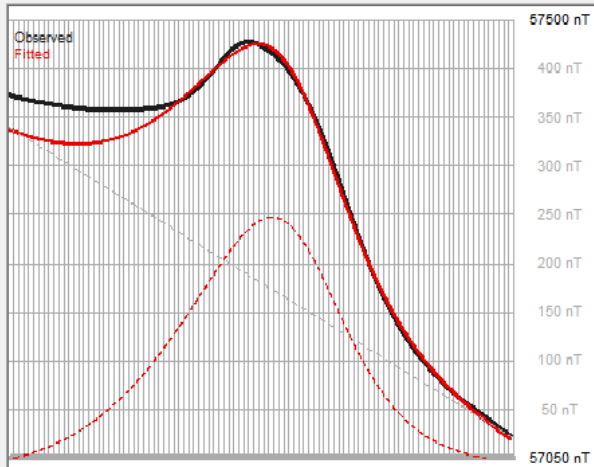
	Model A	Model B	Model C	Model D	Model E
UTM X (m)	583430.75				
UTM Y (m)	6270765.50				
Baseline (nT)	57433.71				
Slope (nT/m)	0.00				
Susc(mSI)	493.60				
Depth (m)	4942.73				
Width (m)	197.27				
Length (m)	27708.80				
Thickness (m)	9021.71				
Dip Angle (°)	149.07				
Offset (m)	2769.58				
Field (nT)	57310.00				
Inclination(°)	76.00				
Declination(°)	18.00				
Konigsberg	0.00				
Inclination(°)	0.00				
Azimuth(°)	0.00				



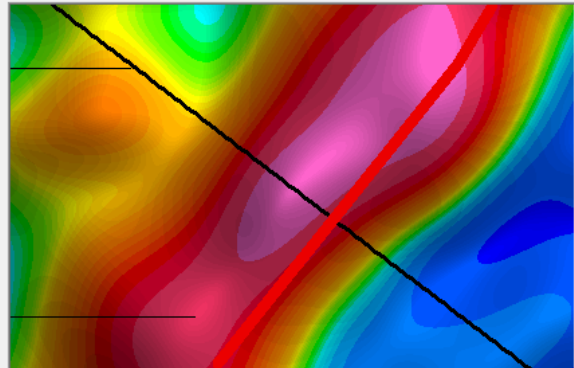
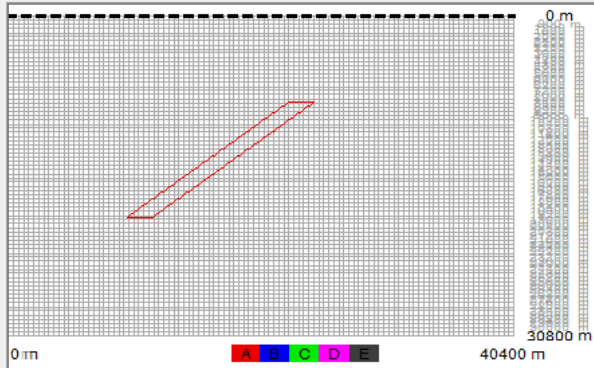
Magnetic MultiMod  
ShaGeophysics.com

**Peace Region**  
Magnetic Model

Model : 8 Line: 110  
PR\_SL5.GRD



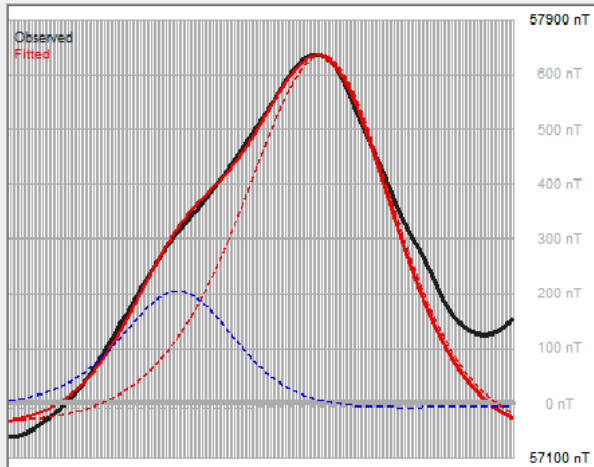
	Model A	Model B	Model C	Model D	Model E
UTM X (m)	628556.31				
UTM Y (m)	6375357.00				
Baseline (nT)	57388.66				
Slope (nT/m)	-0.01				
Susc(mSI)	218.21				
Depth (m)	8320.65				
Width (m)	2027.94				
Length (m)	36417.98				
Thickness (m)	11018.24				
Dip Angle (°)	139.29				
Offset (m)	2384.12				
Field (nT)	57310.00				
Inclination(°)	76.00				
Declination(°)	18.00				
Konigsberg	0.00				
Inclination(°)	0.00				
Azimuth(°)	0.00				



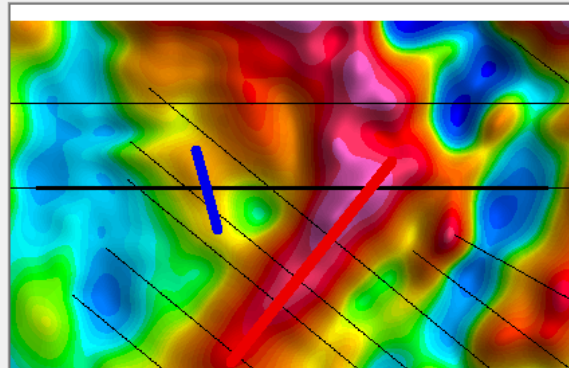
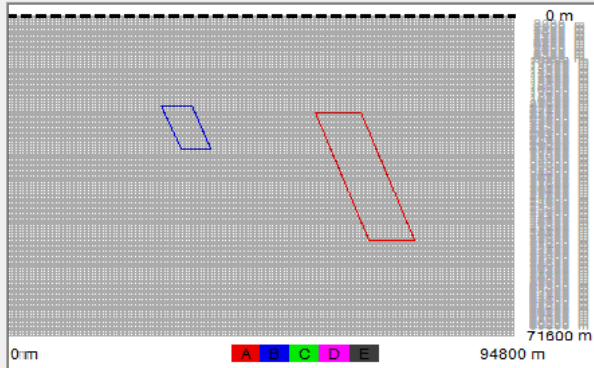
Magnetic MultiMod  
ShaGeophysics.com

**Peace Region**  
Magnetic Model

Model : 9 Line: 190  
PR\_SL5.GRD



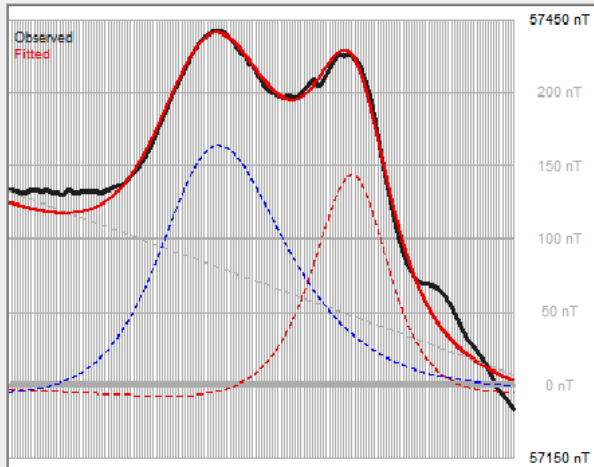
	Model A	Model B	Model C	Model D	Model E
UTM X (m)	559654.19	540492.94			
UTM Y (m)	6350292.00	6363555.00			
Baseline (nT)	57192.18	57192.18			
Slope (nT/m)	0.00	0.00			
Susc(mSI)	788.74	505.83			
Depth (m)	21512.27	20054.94			
Width (m)	6651.32	5422.85			
Length (m)	47488.96	14942.93			
Thickness (m)	28737.18	9511.07			
Dip Angle (°)	74.83	70.03			
Offset (m)	1545.19	1166.34			
Field (nT)	57310.00	57310.00			
Inclination(°)	76.00	76.00			
Declination(°)	18.00	18.00			
Konigsberg	0.00	0.00			
Inclination(°)	0.00	0.00			
Azimuth(°)	0.00	0.00			



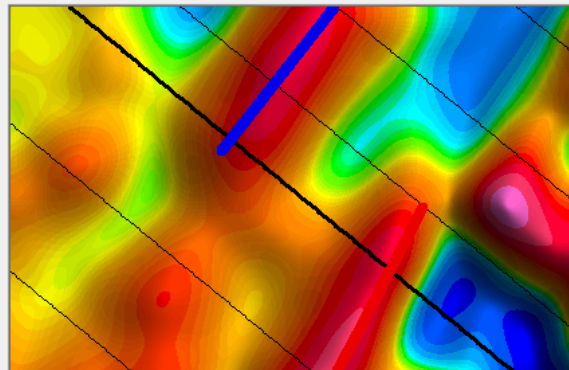
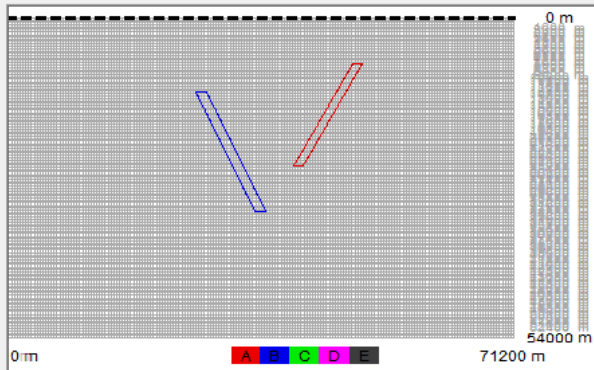
Magnetic MultiMod  
ShaGeophysics.com

**Peace Region**  
Magnetic Model

Model : 10 Line: 150  
PR\_SL5.GRD



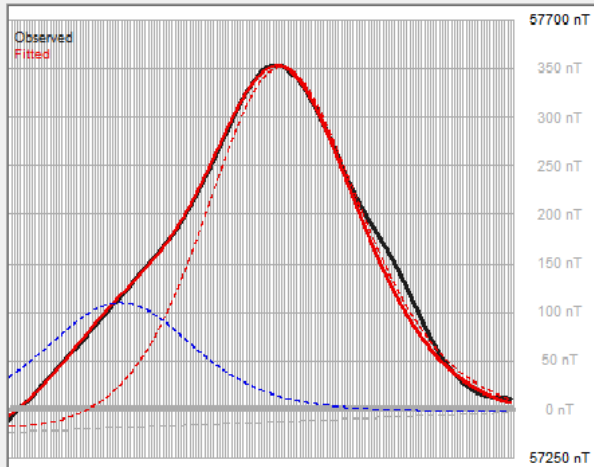
	Model A	Model B	Model C	Model D	Model E
UTM X (m)	582294.62	574249.19			
UTM Y (m)	6271686.00	6299214.50			
Baseline (nT)	57333.12	57333.12			
Slope (nT/m)	0.00	0.00			
Susc(mSI)	171.78	337.04			
Depth (m)	7754.92	12559.34			
Width (m)	1366.97	1562.73			
Length (m)	27710.51	23218.80			
Thickness (m)	17259.05	20000.00			
Dip Angle (°)	115.32	67.39			
Offset (m)	1361.61	267.13			
Field (nT)	57310.00	57310.00			
Inclination(°)	76.00	76.00			
Declination(°)	18.00	18.00			
Konigsberg	0.00	0.00			
Inclination(°)	0.00	0.00			
Azimuth(°)	0.00	0.00			



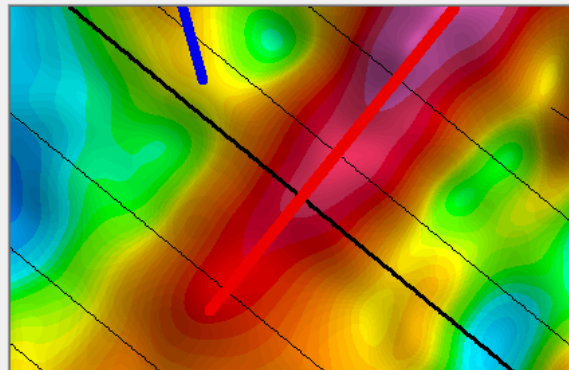
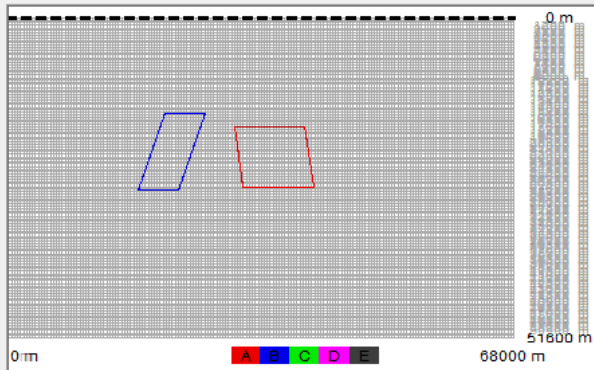
Magnetic MultiMod  
ShaGeophysics.com

**Peace Region**  
Magnetic Model

Model : 11 Line: 100  
PR\_SL5.GRD



	Model A	Model B	Model C	Model D	Model E
UTM X (m)	558418.94	540848.12			
UTM Y (m)	6350037.50	6362305.50			
Baseline (nT)	57276.93	57276.93			
Slope (nT/m)	0.00	0.00			
Susc(mSI)	203.44	235.84			
Depth (m)	17530.11	15376.55			
Width (m)	9454.82	3151.88			
Length (m)	47488.96	14942.93			
Thickness (m)	9735.20	12362.67			
Dip Angle (°)	83.01	99.24			
Offset (m)	401.07	1968.77			
Field (nT)	57310.00	57310.00			
Inclination(°)	76.00	76.00			
Declination(°)	18.00	18.00			
Konigsberg	0.00	0.00			
Inclination(°)	0.00	0.00			
Azimuth(°)	0.00	0.00			



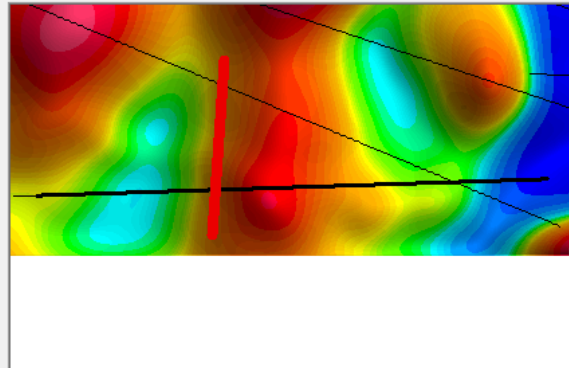
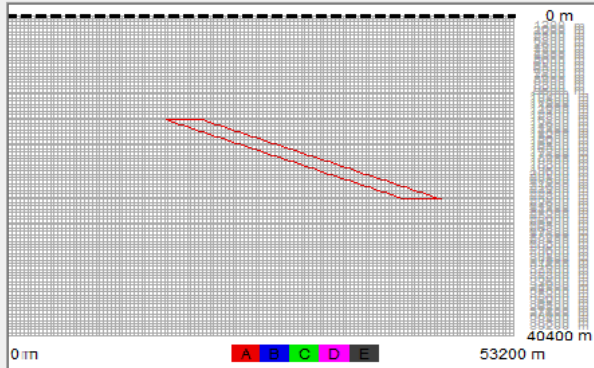
Magnetic MultiMod  
ShaGeophysics.com

**Peace Region**  
Magnetic Model

Model : 12 Line: 70  
PR\_SL5.GRD



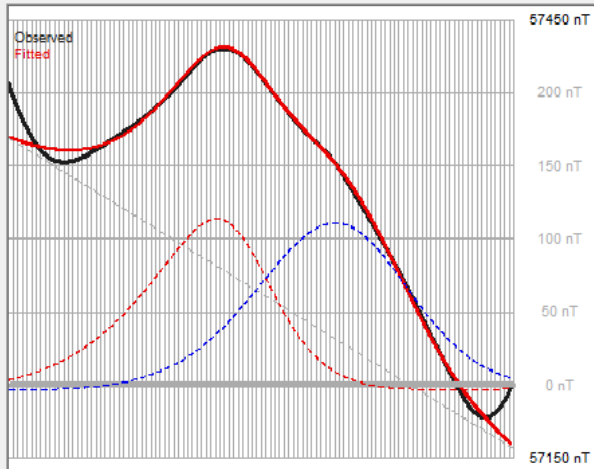
	Model A	Model B	Model C	Model D	Model E
UTM X (m)	542832.81				
UTM Y (m)	6219856.50				
Baseline (nT)	57401.73				
Slope (nT/m)	-0.01				
Susc(mSI)	307.00				
Depth (m)	13202.47				
Width (m)	3762.46				
Length (m)	18024.13				
Thickness (m)	10000.00				
Dip Angle (°)	21.78				
Offset (m)	-6377.87				
Field (nT)	57310.00				
Inclination(°)	76.00				
Declination(°)	18.00				
Konigsberg	0.00				
Inclination(°)	0.00				
Azimuth(°)	0.00				



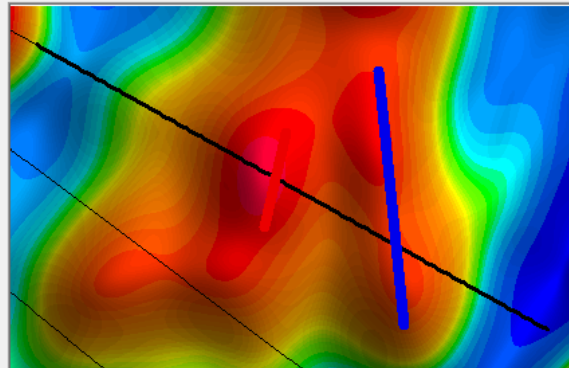
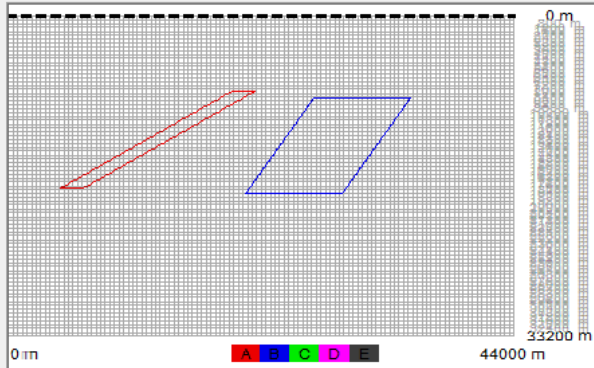
Magnetic MultiMod  
ShaGeophysics.com

**Peace Region**  
Magnetic Model

Model : 13 Line: 30  
PR\_SL5.GRD



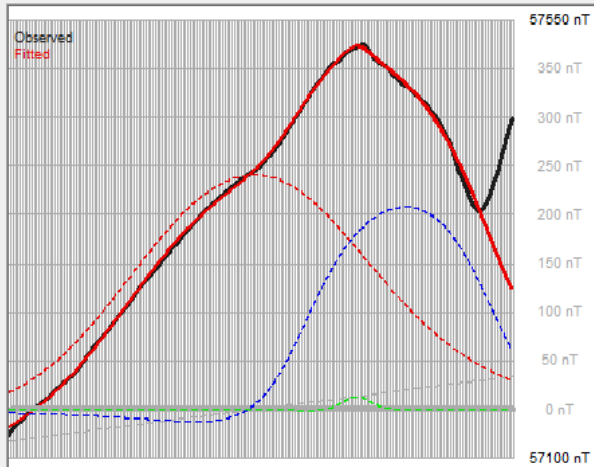
	Model A	Model B	Model C	Model D	Model E
UTM X (m)	606869.19	615576.69			
UTM Y (m)	6343587.00	6342222.50			
Baseline (nT)	57369.12	57369.12			
Slope (nT/m)	0.00	0.00			
Susc(mSI)	236.83	32.43			
Depth (m)	7852.24	8467.94			
Width (m)	1873.44	6889.44			
Length (m)	7125.48	18972.84			
Thickness (m)	10000.00	10000.00			
Dip Angle (°)	145.29	116.11			
Offset (m)	791.70	-245.35			
Field (nT)	57310.00	57310.00			
Inclination(°)	76.00	76.00			
Declination(°)	18.00	18.00			
Konigsberg	0.00	0.00			
Inclination(°)	0.00	0.00			
Azimuth(°)	0.00	0.00			



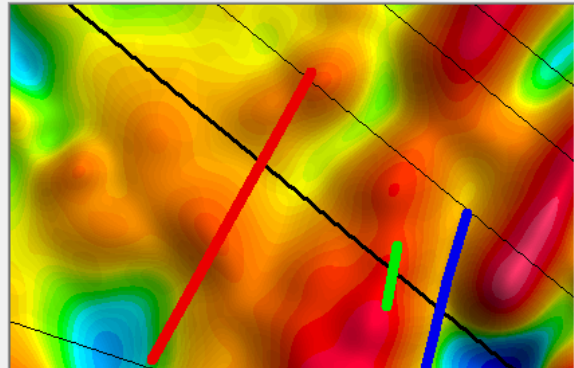
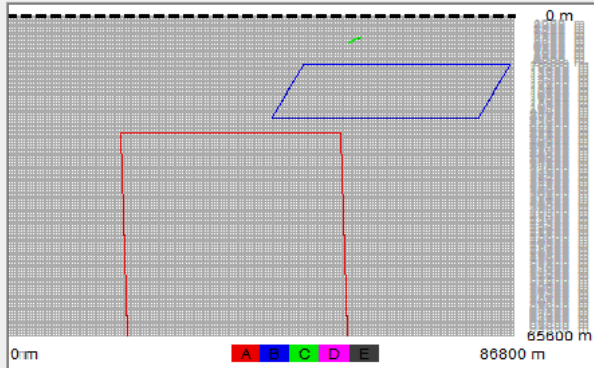
Magnetic MultiMod  
ShaGeophysics.com

**Peace Region**  
Magnetic Model

Model : 14 Line: 40  
PR\_SL5.GRD



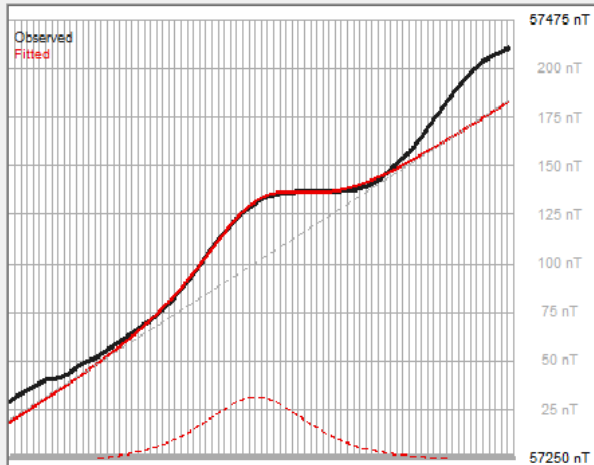
	Model A	Model B	Model C	Model D	Model E
UTM X (m)	539645.31	567501.69	560642.06		
UTM Y (m)	6270733.50	6260800.00	6262956.50		
Baseline (nT)	57117.84	57117.84	57117.84		
Slope (nT/m)	0.00	0.00	0.00		
Susc(mSI)	47.42	31.83	124.65		
Depth (m)	24026.36	10107.22	4392.02		
Width (m)	37246.41	31957.64	317.79		
Length (m)	42797.47	21328.55	8122.00		
Thickness (m)	53545.59	10677.41	1077.21		
Dip Angle (°)	88.39	114.41	145.11		
Offset (m)	-21875.92	9518.94	1319.65		
Field (nT)	57310.00	57310.00	57310.00		
Inclination(°)	76.00	76.00	76.00		
Declination(°)	18.00	18.00	18.00		
Konigsberg	0.00	0.00	0.00		
Inclination(°)	0.00	0.00	0.00		
Azimuth(°)	0.00	0.00	0.00		



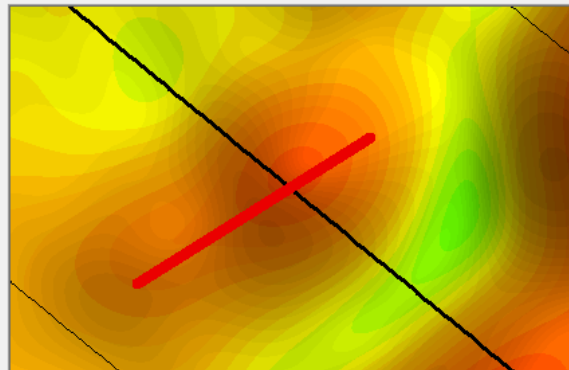
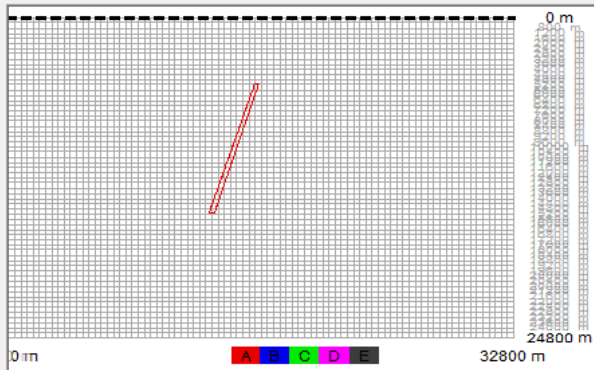
Magnetic MultiMod  
ShaGeophysics.com

**Peace Region**  
Magnetic Model

Model : 15 Line: 120  
PR\_SL5.GRD



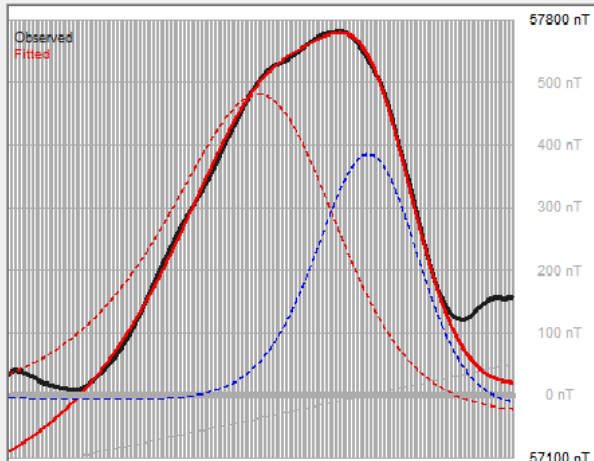
	Model A	Model B	Model C	Model D	Model E
UTM X (m)	549214.56				
UTM Y (m)	6286448.50				
Baseline (nT)	57269.44				
Slope (nT/m)	0.01				
Susc(mSI)	104.18				
Depth (m)	5050.24				
Width (m)	299.27				
Length (m)	13559.15				
Thickness (m)	10000.00				
Dip Angle (°)	105.40				
Offset (m)	700.38				
Field (nT)	57310.00				
Inclination(°)	76.00				
Declination(°)	18.00				
Konigsberg	0.00				
Inclination(°)	0.00				
Azimuth(°)	0.00				



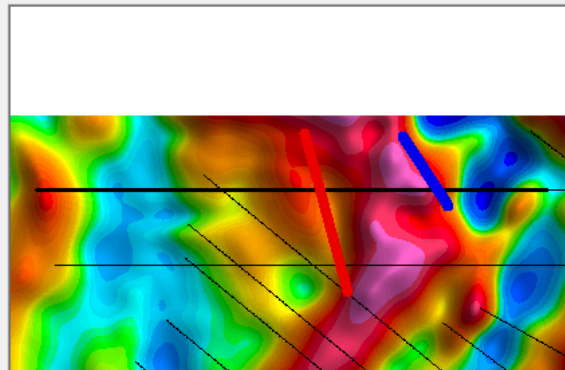
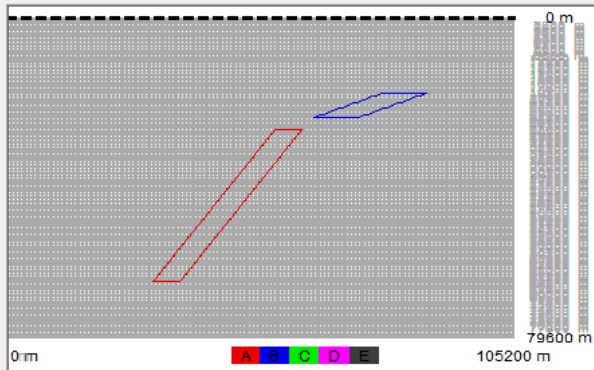
Magnetic MultiMod  
ShaGeophysics.com

**Peace Region**  
Magnetic Model

Model : 16 Line: 110  
PR\_SL5.GRD



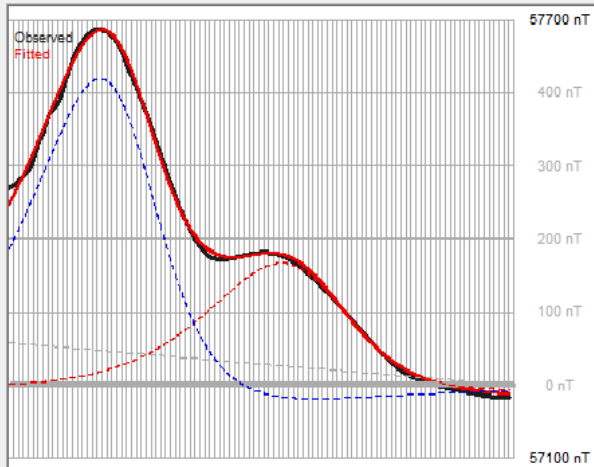
	Model A	Model B	Model C	Model D	Model E
UTM X (m)	554637.62	574988.38			
UTM Y (m)	6374751.50	6383297.00			
Baseline (nT)	57078.43	57078.43			
Slope (nT/m)	0.00	0.00			
Susc(mSI)	904.73	736.77			
Depth (m)	27773.05	18753.73			
Width (m)	5302.99	7639.51			
Length (m)	33493.14	16961.16			
Thickness (m)	37943.95	5932.94			
Dip Angle (°)	122.77	153.44			
Offset (m)	-6853.92	5218.39			
Field (nT)	57310.00	57310.00			
Inclination(°)	76.00	76.00			
Declination(°)	18.00	18.00			
Konigsberg	0.00	0.00			
Inclination(°)	0.00	0.00			
Azimuth(°)	0.00	0.00			



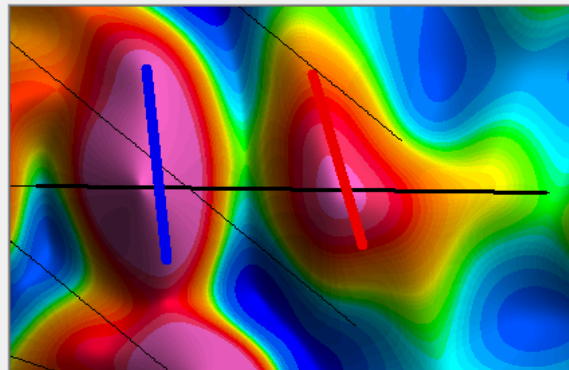
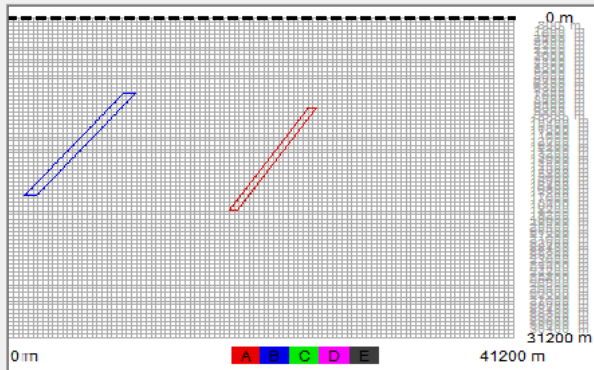
Magnetic MultiMod  
ShaGeophysics.com

**Peace Region**  
Magnetic Model

Model : 17 Line: 10  
PR\_SL5.GRD



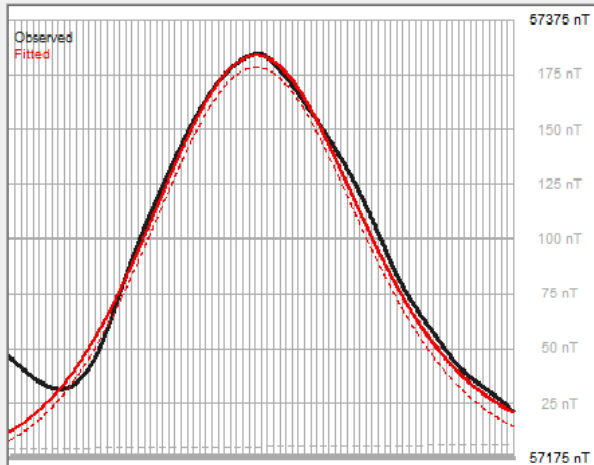
	Model A	Model B	Model C	Model D	Model E
UTM X (m)	615900.88	601483.75			
UTM Y (m)	6246299.50	6245962.00			
Baseline (nT)	57258.48	57258.48			
Slope (nT/m)	0.00	0.00			
Susc(mSI)	618.10	780.49			
Depth (m)	8708.04	7357.36			
Width (m)	609.32	908.13			
Length (m)	14196.37	15217.09			
Thickness (m)	10000.00	10000.00			
Dip Angle (°)	121.82	128.77			
Offset (m)	198.81	1003.47			
Field (nT)	57310.00	57310.00			
Inclination(°)	76.00	76.00			
Declination(°)	18.00	18.00			
Konigsberg	0.00	0.00			
Inclination(°)	0.00	0.00			
Azimuth(°)	0.00	0.00			



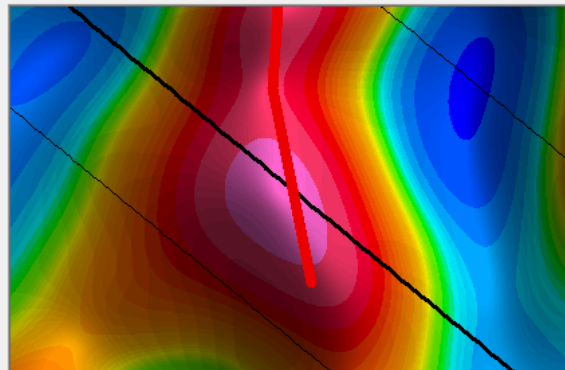
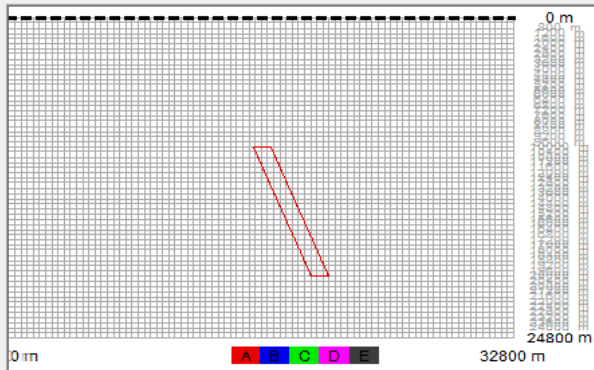
Magnetic MultiMod  
ShaGeophysics.com

Peace Region  
Magnetic Model

Model : 18 Line: 180  
PR\_SL5.GRD



	Model A	Model B	Model C	Model D	Model E
UTM X (m)	612680.44				
UTM Y (m)	6303447.50				
Baseline (nT)	57179.01				
Slope (nT/m)	0.00				
Susc(mSI)	702.91				
Depth (m)	10003.79				
Width (m)	717.22				
Length (m)	13938.17				
Thickness (m)	10000.00				
Dip Angle (°)	76.68				
Offset (m)	54.15				
Field (nT)	57310.00				
Inclination(°)	76.00				
Declination(°)	18.00				
Konigsberg	0.00				
Inclination(°)	0.00				
Azimuth(°)	0.00				



Magnetic MultiMod  
ShaGeophysics.com

**Peace Region**  
Magnetic Model

Model : 19 Line: 60  
PR\_SL5.GRD